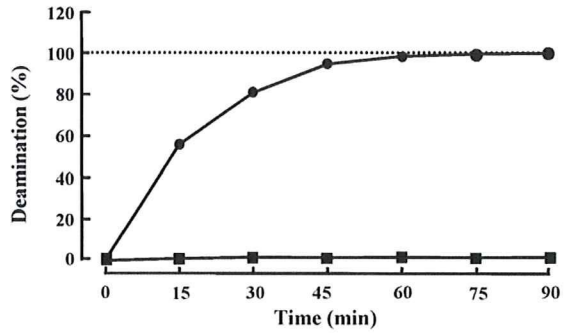

Fig. 2. Stability of EFdA following exposure to ADA. EdA or EFdA was incubated with ADA as described in Section 2. The deamination of adenine to inosine was analyzed by HPLC at indicated time points. The data represent the percent of starting compound (EdA; circle, EFdA; box) that was not deaminated by ADA.

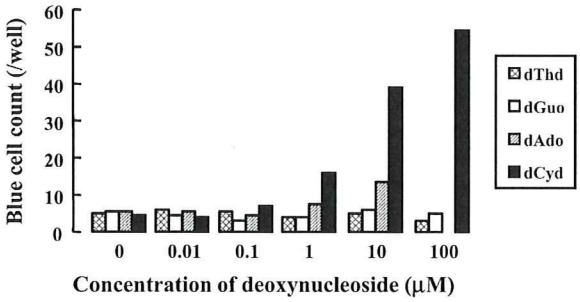

Fig. 3. Reversal of the antiviral activity of EFdA in the presence of 2′-deoxynucleosides. Each 2′-deoxynucleoside was added to the medium with serial dilution in the presence of EFdA (3.5 nM). The effect on EFdA activity was determined by the MAGI assay. An ADA inhibitor, dCF, was used during dA competition.

activity of EFdA. We could observe a slight reversal of the antiviral effect by addition of 10 μM dA with dCF. Effect of 100 μM dA could not be examined because of its cytotoxicity. It should be noted that all other tested analogs, including EFddA and EFd4A, were also reversed by the addition of dC (data not shown).

To confirm that the cellular dCK mediates the phosphorylation of EFdA, we examined the antiviral activity of EFdA in the HT-1080, dCK-deficient HT-1080/Ara-C^r (Obata et al., 2001), and dCK-transduced HT-1080/Ara-C^r cell lines. As expected, the antiviral activity of EFdA was markedly reduced in HT-1080/Ara-C^r cells (677-fold), but restored in dCK-transfected cells (Table 4). The same activity profile was observed with ddC, which is also phosphorylated by dCK (Starnes and Cheng, 1987). In contrast, AZT showed comparable activity among three cell lines, since it is known to be phophorylated mainly by thymidine kinase (Furman et al., 1986). Although dCK appears to be the main enzyme responsible for mono-phosphorylation of EFdA, other kinases, such as adenosine/deoxyadenosine kinases, may be partially involved in mono-phosphorylation of EFdA, especially since weak reduction in antiviral activity of EFdA was observed in addition of dA in high concentrations. Moreover, even in dCK-deficient HT-1080/Ara-C^r cells, EFdA exerted moderate antiviral activity. Hence, while it is possible that other kinases may be contributing to a smaller extent to the phosphorylation of EFdA, it appears that dCK is the enzyme that primarily phosphorylates this inhibitor.

3.6. Resistance to EFdA

In order to elucidate the mechanism of drug resistance to 4′-E analogs, we selected variants resistant to EdA, a parental compound of EFdA with the dose escalating methods (Nameki et al., 2005). After 58 passages in the presence of EdA, the resistant variants were obtained. Sequence analysis of the entire RT region revealed that a novel combination of mutations, I142V/T165R/M184V was introduced. Similar mutations (I119S/T165A/M184V) were observed in a Ed4T-resistant variant (Nitanda et al., 2005). Hence, we generated infectious clones containing these mutations and tested the antiviral activity of 4′-E analogs against them (Table 2). Mutation in T165, either Arg or Ala, enhanced the resistance against EdA, EFdA, and ECldA in the presence of the M184V mutation. Similar resistance profiles were observed for the I142V/M184V mutations. Furthermore, the triple mutant HIV-$1_{I142V/T165R/M184V}$ had the highest resistance among all tested variants. On the other hand, I142V or T165R alone did not affect the antiviral activity of EFdA or ECldA, although EdA or EFddA showed slightly decreased susceptibility. These results suggest that M184V appears to be the main mutation responsible for 4′-E analog resistance, and the addition of I142V and/or T165R augments the effect of M184V.

3.7. Replication of resistant HIV-1

For acquisition of high-level resistance to EFdA as well as EdA, three mutations, I142V, T165R, and M184V were required as described above. To examine the effect of the mutations on the viral replication kinetics we performed an assay that follows production of p24 gag antigen. All clones with M184V showed reduced replication kinetics (Fig. 4A), consistent with the reports that introduction of M184V markedly impairs replication kinetics (Wainberg et al., 1996; Yoshimura et al., 1999). Introduc-

Table 4
The effect of dCK expression on the EFdA antiviral activity[a]

Cell	EC_{50} (μM)[b]		
	AZT	ddC	EFdA
HT-1080	0.0032 ± 0.001	0.75 ± 0.22	0.00031 ± 0.0001
HT-1080/Ara-C^r	0.0027 ± 0.0005 (0.84)	84 ± 15 (112)	0.21 ± 0.03 (677)
HT-1080/Ara-C^r/dCK	0.0025 ± 0.00074 (0.78)	0.51 ± 0.16 (0.68)	0.000098 ± 0.000034 (0.32)

[a] SEAP activity in the culture supernatants were determined on day 2 after virus infection.
[b] The data shown are mean ± S.D. and fold increase in EC_{50} compared to HT-1080 is shown in parentheses.

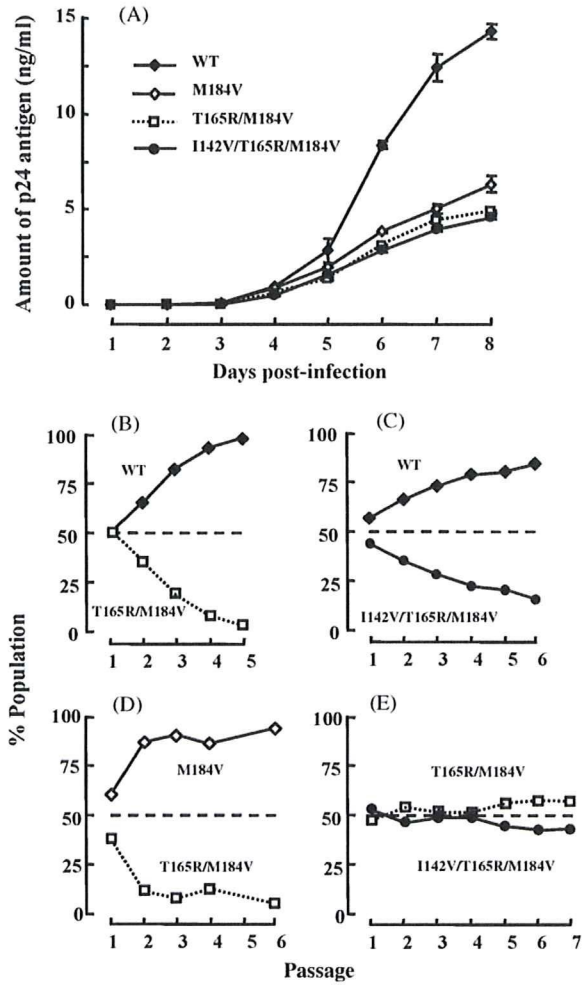

Fig. 4. Replication kinetics of HIV-1 clones with mutations. Production of p24 antigen in culture supernatant was determined with a commercially available p24 antigen kit. Profiles of replication kinetics (p24 production) of HIV-1_{WT} (closed diamonds), HIV-1_{M184V} (open diamonds), HIV-$1_{T165R/M184V}$ (open squares with broken line) and HIV-$1_{I142V/T165R/M184V}$ (open circles) were determined with MT-2 (A). Representative results from three independent triplicate determinations of p24 production with newly titrated viruses are shown. MT-2 cells were infected simultaneously with equal amounts of two HIV-1 clones to be compared. At each passage (5–6 days) the proviral sequences were determined and the percent population of each clone is reported at different passage; competition of WT and T165R/M184V (B); competition of WT with I142V/T165R/M184V (C); competition of M184V with T165R/M184V (D), and competition of T165R/M184V with I142V/T165R/M184V (E). At least two independent CHRAs were performed and are shown the representative results.

tion of T165R or I142V/T165R mutations in an M184V background (HIV-$1_{T165R/M184V}$ or HIV-$1_{I142V/T165R/M184V}$, respectively) further impaired HIV replication compared to HIV-1_{M184V}. I142V which enhanced EFdA resistance of HIV-$1_{T165R/M184V}$ (Table 2) conferred no replication rescue of HIV-$1_{T165R/M184V}$. To determine detailed replication kinetics, we performed CHRA which compares qualitatively viral replication. As shown in Fig. 4A, HIV-$1_{T165R/M184V}$ and HIV-$1_{I142V/T165R/M184V}$ showed reduced replication kinetics compared to HIV-1_{WT} (Fig. 4B and C). Replication kinetics ofHIV-$1_{I142V/T165R/M184V}$ was comparable to that of HIV-$1_{T165R/M184V}$, which showed further reduced replication kinetics compared to HIV-1_{M184V} (Fig. 4D and E). In another experiment, replication of HIV-$1_{I142V/T165R/M184V}$ was slightly decreased compared to HIV-$1_{T165R/M184V}$ (data not shown). These results suggest that introduction of three EdA mutations that also confers EFdA resistance impaired replication of HIV-1 in much greater extent compared to that of M184V.

4. Discussion

At present, HIV-1 variants containing NRTI-resistance mutations are widely observed not only in NRTI-experienced but also in NRTI-naïve patients. In such cases treatment failure is sometimes observed within short periods. The NRTI tenofovir, appears to be more effective against drug-experienced HIV-1 strains (Srinivas and Fridland, 1998). Unlike the other clinically available NRTIs, tenofovir has highly flexible acyclic ribose ring without a 3′-OH. Structural studies have suggested that the compact size of this inhibitor may contribute to the absence of highly resistant mutant strains against tenofovir (Tuske et al., 2004). Despite its unique structural profile, tenofovir is similar to other NRTIs in that it also lacks a 3′-OH group.

In contrast, the highly active 4′-E analogs such as EFdA retain the 3′-OH group of the canonical dNTP substrate. Similar to other NRTIs, they are also phosphorylated by cellular enzymes to their TP active form, which in turn serves as a substrate for HIV RT that incorporates them in an elongating primer during DNA synthesis. Following incorporation, replication is further inhibited by chain termination, although the specific mechanism of chain termination remains to be elucidated. Despite the fact that the 4′-E analogs have a 3′-OH like canonical dNTP substrates, cellular polymerases are likely to discriminate against these analogs, and not incorporate them during cellular DNA polymerization, as suggested by *in vitro* experiments with mitochondrial polymerase γ (Nakata et al., 2007). Alternatively, it is also possible that cellular proofreading systems excise the 4′-E analogs after their incorporation into cellular DNA.

The 3′-OH also plays an important role in phosphorylation of EdA analogs. Based on crystallographic results Sabini et al. reported that the interaction between 3′-OH of nucleosides and catalytic site of dCK was important for efficient nucleoside phosphorylation (Sabini et al., 2003). Alternatively, it is possible that the EFddA and EFd4A nucleosides that lack 3′-OH are poor substrates for HIV RT. The substitution at the 2-position of the purine base is also likely to contribute to highly potent *in vivo* activity of EF- or EClda, possibly by preventing deamination of the inhibitor by ADA. ADA deaminates the adenine base into inosine, which is a poor substrate for cellular kinases. Similar ADA resistance has been reported for 2′-deoxy-2-chloroadenosine, a chemotherapeutic agent against hairy cell leukemia and chronic lymphocytic leukemia (Carson et al., 1980). ADA resistance may contribute to a longer intracellular half-life for EFdA-TP as compared to that of AZT (Nakata et al., 2007), indicating that substitution of 2-position plays an important role in sustained activity. When CEM cells were exposed to AZT or EFdA at concen-

tration of 0.1 μM, amounts of corresponding intracellular TP-forms were comparable (Nakata et al., 2007). However, inhibitory effect of EFdA in MT-4 and MAGI cells was approximately 40- and 15-fold superior compared to that of AZT (Tables 1 and 2). Taken together, HIV-1 RT appears to preferentially incorporate EFdA-TP compared to AZT-TP, although detailed enzymatic confirmation is needed. The parental EdA also seems to be a good substrate for HIV-1 RT; however, it may be subjected to deamination, resulting in comparable activity to AZT.

There are at least two mechanisms by which HIV RT can become resistant to NRTIs: first, HIV RT can acquire mutations at, or close to the dNTP-binding site, such that help it discriminate against NRTI-triphosphates, while it retains its ability to recognize the normal dNTP substrates (Huang et al., 1998). In the case of M184V/I the discrimination is based on steric conflict between a part of the inhibitor (the sulfur atom of the thioxolane ring in the case of 3TC), and the β-branched side chain of Val or Ile at the mutation site (Sarafianos et al., 1999). Mutations at other residues of the dNTP-binding site are responsible for discrimination of dideoxynucleosides from dNTPs during both the substrate-recognition (Martin et al., 1993) and the catalytic steps (Deval et al., 2002; Selmi et al., 2001). The other mechanism of NRTI resistance is based on an excision reaction (phosphorolysis) that unblocks NRTI-terminated primers using a molecule of ATP as the pyrophosphate donor (Meyer et al., 1999). The product of this reaction is a dinucleoside tetraphosphate and an unblocked primer that can continue viral DNA synthesis. In this case, the role of resistance mutations is to optimize binding of an ATP molecule that is used for the nucleophilic attack at the primer terminus. Most of AZT resistance as well as multi-NRTI resistance of RT with insertions at the fingers subdomain are thought to be based on an ATP-based unblocking mechanism. The insertions in RT destabilize the normally stable ternary complex (RT/template-primer/dNTP) and facilitate the ATP-mediated pyrophospholysis (Boyer et al., 2002). The fingers insertion mutant can excise all nucleotide analogs, with various degrees of efficiency.

Our molecular modeling studies are consistent with a mechanism of resistance to 4′-E analogs that involves steric hindrance between the 4′-E group of the inhibitors and the side chain of V184, reminiscent of the resistance mechanism to 3TC. While a single M184V mutation confers strong resistance to 3TC (>100-fold), it causes only moderate (8- to 13-fold) resistance to EFdA and ECldA (Table 2). This is consistent with our molecular modeling analysis where the bulky and rigid 4′-E moiety appears to cause some steric hindrance with the Val or Ile side chain at position 184 during incorporation of the 4′-E nucleotides by the M184V enzyme (Fig. 5). The steric interaction appears to be stronger during incorporation of 3TC-TP (Fig. 5E) than EFdA-TP (Fig. 5C). Interestingly, the M184V mutation appears to confer stronger resistance to 4′-methyl substituted nucleotides, than to the 4′-ethynyl substituted nucleotides (Kodama et al., 2001). The decreased resistance of 4′-ethynyl substituted compounds may be in part the result of compensatory favorable interactions of the longer ethynyl group with residues of the dNTP binding site, including Y115 and D185. Such interactions may moderate the effect of the steric interactions of the 4′-ethynyl with residue V184 in the M184V mutant. Resistance of M184V to dideoxy-derivatives such as EFddA was unexpectedly high (84-fold). Although we cannot explain the detailed mechanism of the difference in resistance, it is possible that the presence of a 3′-OH in the EFdA (but not in the EFddA and EFd4A) results in more stabilizing interactions with residues such as Q151 that compensate for the steric hindrance by M184V (Fig. 5D). Hence, EFddA and EFd4A may be easier to push out of the binding pocket than analogs with a 3′-OH. For stronger resistance to 4′-E-2-halo-dAs, other mutations at positions 142 and 165 in addition to the M184V are required (Table 2) to substantially decrease inhibitor binding. It should be noted that the T165R/M184V mutations were also observed during induction of resistant variants to parental compound EdA. Nitanda et al. also reported that resistant variants for 4′-Ed4T contain M184V with T165A (Nitanda et al., 2005). As shown in Fig. 5A, the effect of the T165R mutation seems to be through the loss of a hydrogen bond between the side chain of Q182 and the side chain OH moiety of T165. Instead, there may be a hydrogen bond between C=O of the main chain of 184 and Q182 in the case of T165R/A, which would affect the positioning of the residue in position 184. Interestingly, HIV-2 has an Arg residue at position 165, whereas HIV-1 has Thr. We could not find decreased susceptibility in HIV-1_{T165R} or HIV-2, indicating that R165 becomes relevant only when Val is at the 184 position. When this residue is Met (T165R in M184 background), resistance is not affected substantially (1.5- to 2-fold resistance, Table 2) because of the flexibility of the Met side chain. However, when the 184 residue is Val (T165R/M184V), the position of 184 may be affected in a way that exacerbates the steric interactions between the ethynyl group of the incoming EFdA and the side chain of V184, resulting in resistance to EFdA and the other 4′-E analogs (13–27-fold resistance, Table 2). At this point it is not clear why the I142V mutation further augmented the effects of M184V and T165R. Finally, as shown in Fig. 5B, there are no apparent substantial steric problems for binding of EFdA to HIV-$1_{M41L/T69SSG/T215Y}$ RT, and the enzyme–inhibitor interactions are likely to be similar to those with dNTP and consistent with the relatively low resistance observed with this variant (Table 2) that is known to cause strong excision-based NRTI resistance. Crystallographic studies with the RT resistant variants complexed with the inhibitors should provide more insights into the mechanism of resistance.

The M184V, one of three mutations associated with EFdA resistance, develops rapidly under therapy with 3TC and has been reported to alter several profiles of RT function, including decreased RT processivity (Back et al., 1996), reduced nucleotide-dependent primer unblocking (Gotte et al., 2000), and increased fidelity (Wainberg et al., 1996). These profiles result in impaired viral fitness, hypersensitivity to other NRTIs, especially AZT (Larder et al., 1995), and delayed appearance of mutations, respectively. Our results show that modest resistance to EdA comes at a significant cost for the virus: The I142V and T165R mutations reduced even further viral replication kinetics of M184V-containing virus. Furthermore, the virus containing these mutations retains the AZT hyper-susceptibility which is induced by

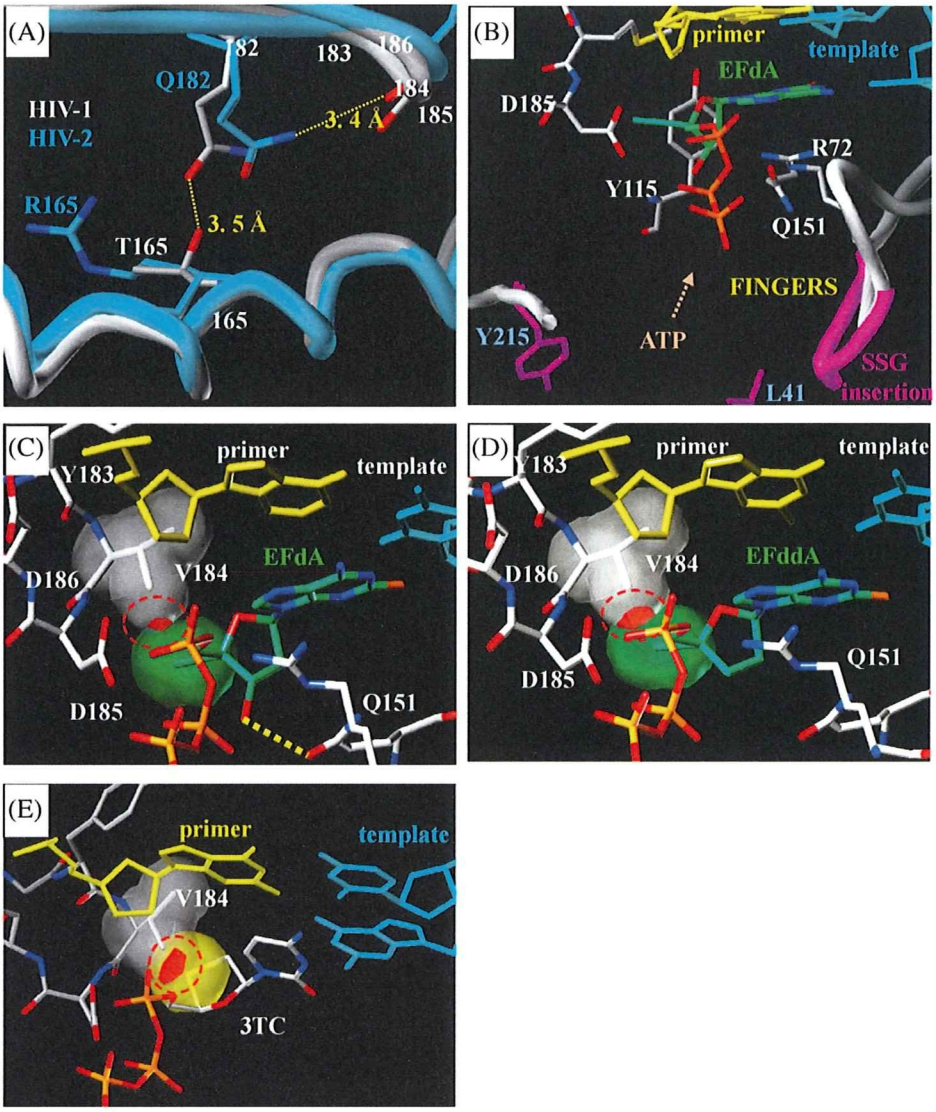

Fig. 5. Structural modeling of reverse transcriptase and compounds. (A) Superposition of the polymerase active sites of HIV-1 (gray) and HIV-2 (magenta) reverse transcriptases. Q182 makes a hydrogen bond with T165 in HIV-1. In the T165R mutant of HIV-1, the arginine side chain is expected to have a conformation similar to the one observed for R165 in HIV-2. In this context, Arg does not make a hydrogen bond with the side chain of residue 182 that may now interact with the main chain carbonyl of M184, which is at the immediate vicinity of the inhibitor-binding site. Such interaction may explain how the T165R mutation exacerbates the role of the M184V mutation in resistance to EFdA. (B) Proposed interactions of EFdA-triphosphate (TP) at the polymerase active site of the "fingers-insertion" NRTI-resistant HIV-1 RT, carrying the M41L/T69SSG/T215Y mutations. Possible steric interactions between the 4′-E group of EFdA-TP (C) or EFddA-TP (D) and the sulfur (S) of the pseudosugar ring of 3TC-TP (E). Van der Waals surfaces of 4′-E group (C and D) and S at sugar ring (E) are indicated in green and yellow. Possible steric interactions are shown as overalap of Van der Waal volumes of interacting atoms (in red).

M184V (Table 2), although further experiments are needed. These results suggest that the I142V and T165R mutations simply enhance resistance of M184V RT to EdA rather than optimize the viral fitness of the M184V virus. The increased cost for the virus to overcome inhibition pressure by EdA may have significant clinical benefits in the treatment of HIV infections.

Since EFdA is initially phosphorylated mainly by dCK and its activity was attenuated by addition of dC (data not shown), it is likely that dC analogs, such as 3TC and emtricitabine (FTC) that are mainly phosphorylated by dCK would act as a competitor of EFdA phosphorylation. However, one of dC analogs, apricitabine (ATC) showed little competition for the intracellular phosphorylation of 3TC and FTC (Bethell et al., 2007). Thus, interaction of NRTIs using identical phosphorylation enzymes should be carefully examined.

In conclusion, we have shown that the 2-halogen substituted EdAs have exceptionally potent subnanomolar antiviral activities. The 2-F substituted analog exhibited the highest potency and had a selectivity index significantly improved over that of approved NRTIs. In fact, results from our parallel studies with mice show no toxicity of EFdA (data not shown). The earlier studies also showed that a

parental nucleoside, EdA was not toxic in mice (Kohgo et al., 2004). The half-life of the intracellular TP form of EFdA is substantially extended (~17 h) compared to that of AZT (~3 h) (Nakata et al., 2007), suggesting that it may be possible to administer these inhibitors once a day. Further investigation may lead to their development as potential therapeutics against HIV infections.

Acknowledgements

We would like to thank S. Oka, T. Sasaki, M. Emerman, J. Overbaugh, K.-T. Jeang, M. Baba for providing HIV-1 clinical isolates, HT-1080 and HT-1080/Ara-C^r cell lines, HeLa-CD4-LTR/β-gal cells and HeLa-CD4/CCR5-LTR/β-gal cells through the AIDS Research and Reference Reagent Program, Division of AIDS, National Institute of Allergy and Infectious Diseases (Bethesda, MD), pNL101, pLTR-SEAP-puro, respectively. A.K. is supported by the 21st Century COE program of the ministry of Education, Culture, Sports, Science, and Technology. This work was supported by a grant for the promotion of AIDS Research from the Ministry of Health, Labor, and Welfare (E.K. and M.M.), a grant for Research for Health Sciences Focusing on Drug Innovation from The Japan Health Sciences Foundation (E.K. and M.M.).

References

Back NK, Nijhuis M, Keulen W, Boucher CA, Oude Essink BO, van Kuilenburg AB, et al. Reduced replication of 3TC-resistant HIV-1 variants in primary cells due to a processivity defect of the reverse transcriptase enzyme. EMBO J 1996;15(15):4040–9.

Bethell R, De Muys J, Lippens J, Richard A, Hamelin B, Ren C, et al. In vitro interactions between apricitabine and other deoxycytidine analogues. Antimicrob Agents Chemother 2007;51(8):2948–53.

Bhalla KN, Li GR, Grant S, Cole JT, MacLaughlin WW, Volsky DJ. The effect in vitro of 2′-deoxycytidine on the metabolism and cytotoxicity of 2′,3′-dideoxycytidine. AIDS 1990;4(5):427–31.

Boyer PL, Sarafianos SG, Arnold E, Hughes SH. Nucleoside analog resistance caused by insertions in the fingers of human immunodeficiency virus type 1 reverse transcriptase involves ATP-mediated excision. J Virol 2002;76(18):9143–51.

Carson DA, Wasson DB, Kaye J, Ullman B, Martin Jr DW, Robins RK, et al. Deoxycytidine kinase-mediated toxicity of deoxyadenosine analogs toward malignant human lymphoblasts in vitro and toward murine L1210 leukemia in vivo. Proc Natl Acad Sci USA 1980;77(11):6865–9.

De Clercq E. The role of non-nucleoside reverse transcriptase inhibitors (NNRTIs) in the therapy of HIV-1 infection. Antiviral Res 1998;38(3):153–79.

Deval J, Selmi B, Boretto J, Egloff MP, Guerreiro C, Sarfati S, et al. The molecular mechanism of multidrug resistance by the Q151M human immunodeficiency virus type 1 reverse transcriptase and its suppression using alpha-boranophosphate nucleotide analogues. J Biol Chem 2002;277(44):42097–104.

Dutschman GE, Grill SP, Gullen EA, Haraguchi K, Takeda S, Tanaka H, et al. Novel 4′-substituted stavudine analog with improved anti-human immunodeficiency virus activity and decreased cytotoxicity. Antimicrob Agents Chemother 2004;48(5):1640–6.

Furman PA, Fyfe JA, St Clair MH, Weinhold K, Rideout JL, Freeman GA, et al. Phosphorylation of 3′-azido-3′-deoxythymidine and selective interaction of the 5′-triphosphate with human immunodeficiency virus reverse transcriptase. Proc Natl Acad Sci USA 1986;83(21):8333–7.

Gotte M, Arion D, Parniak MA, Wainberg MA. The M184V mutation in the reverse transcriptase of human immunodeficiency virus type 1 impairs rescue of chain-terminated DNA synthesis. J Virol 2000;74(8):3579–85.

Haraguchi K, Takeda S, Tanaka H, Nitanda T, Baba M, Dutschman GE, et al. Synthesis of a highly active new anti-HIV agent 2′,3′-didehydro-3′-deoxy-4′-ethynylthymidine. Bioorg Med Chem Lett 2003;13(21):3775–7.

Huang H, Chopra R, Verdine GL, Harrison SC. Structure of a covalently trapped catalytic complex of HIV-1 reverse transcriptase: implications for drug resistance. Science 1998;282(5394):1669–75.

Jeang KT, Chun R, Lin NH, Gatignol A, Glabe CG, Fan H. In vitro and in vivo binding of human immunodeficiency virus type 1 Tat protein and Sp1 transcription factor. J Virol 1993;67(10):6224–33.

Kajiwara K, Kodama E, Matsuoka M. A novel colorimetric assay for CXCR4 and CCR5 tropic human immunodeficiency viruses. Antivir Chem Chemother 2006;17(4):215–23.

Kimpton J, Emerman M. Detection of replication-competent and pseudotyped human immunodeficiency virus with a sensitive cell line on the basis of activation of an integrated beta-galactosidase gene. J Virol 1992;66(4):2232–9.

Kodama EI, Kohgo S, Kitano K, Machida H, Gatanaga H, Shigeta S, et al. 4′-Ethynyl nucleoside analogs: potent inhibitors of multidrug-resistant human immunodeficiency virus variants in vitro. Antimicrob Agents Chemother 2001;45(5):1539–46.

Kohgo S, Yamada K, Kitano K, Iwai Y, Sakata S, Ashida N, et al. Design, efficient synthesis, and anti-HIV activity of 4′-*C*-cyano- and 4′-*C*-ethynyl-2′-deoxy purine nucleosides. Nucleosides Nucleotides Nucleic Acids 2004;23(4):671–90.

Kosalaraksa P, Kavlick MF, Maroun V, Le R, Mitsuya H. Comparative fitness of multi-dideoxynucleoside-resistant human immunodeficiency virus type 1 (HIV-1) in an In vitro competitive HIV-1 replication assay. J Virol 1999;73(7):5356–63.

Larder BA, Kemp SD, Harrigan PR. Potential mechanism for sustained antiretroviral efficacy of AZT-3TC combination therapy. Science 1995;269(5224):696–9.

Little SJ, Holte S, Routy JP, Daar ES, Markowitz M, Collier AC, et al. Antiretroviral-drug resistance among patients recently infected with HIV. N Engl J Med 2002;347(6):385–94.

Martin JL, Wilson JE, Haynes RL, Furman PA. Mechanism of resistance of human immunodeficiency virus type 1 to 2′,3′-dideoxyinosine. Proc Natl Acad Sci USA 1993;90(13):6135–9.

Meyer PR, Matsuura SE, Mian AM, So AG, Scott WA. A mechanism of AZT resistance: an increase in nucleotide-dependent primer unblocking by mutant HIV-1 reverse transcriptase. Mol Cell 1999;4(1):35–43.

Mitsuya H, Weinhold KJ, Furman PA, St Clair MH, Lehrman SN, Gallo RC, et al. 3′-Azido-3′-deoxythymidine (BW A509U): an antiviral agent that inhibits the infectivity and cytopathic effect of human T-lymphotropic virus type III/lymphadenopathy-associated virus in vitro. Proc Natl Acad Sci USA 1985;82(20):7096–100.

Miyake H, Iizawa Y, Baba M. Novel reporter T-cell line highly susceptible to both CCR5- and CXCR4-using human immunodeficiency virus type 1 and its application to drug susceptibility tests. J Clin Microbiol 2003;41(6):2515–21.

Nakata H, Amano M, Koh Y, Kodama E, Yang G, Bailey CM, et al. Activity against Human Immunodeficiency Virus Type 1, intracellular metabolism, and effects on human DNA polymerases of 4′-ethynyl-2-fluoro-2′-deoxyadenosine. Antimicrob Agents Chemother 2007;51(8):2701–8.

Nameki D, Kodama E, Ikeuchi M, Mabuchi N, Otaka A, Tamamura H, et al. Mutations conferring resistance to human immunodeficiency virus type 1 fusion inhibitors are restricted by gp41 and Rev-responsive element functions. J Virol 2005;79(2):764–70.

Nitanda T, Wang X, Kumamoto H, Haraguchi K, Tanaka H, Cheng YC, et al. Anti-human immunodeficiency virus type 1 activity and resistance profile of 2′,3′-didehydro-3′-deoxy-4′-ethynylthymidine in vitro. Antimicrob Agents Chemother 2005;49(8):3355–60.

Obata T, Endo Y, Tanaka M, Uchida H, Matsuda A, Sasaki T. Deletion mutants of human deoxycytidine kinase mRNA in cells resistant to antitumor cytosine nucleosides. Jpn J Cancer Res 2001;92(7):793–8.

Ohrui H. 2′-Deoxy-4′-*C*-ethynyl-2-fluoroadenosine, a nucleoside reverse transcriptase inhibitor, is highly potent against all human immunodeficiency viruses type 1 and has low toxicity. Chem Rec 2006;6(3):133–43.

Palella Jr FJ, Delaney KM, Moorman AC, Loveless MO, Fuhrer J, Satten GA, et al. Declining morbidity and mortality among patients with advanced human immunodeficiency virus infection. HIV Outpatient Study Investigators. N Engl J Med 1998;338(13):853–60.

Sabini E, Ort S, Monnerjahn C, Konrad M, Lavie A. Structure of human dCK suggests strategies to improve anticancer and antiviral therapy. Nat Struct Biol 2003;10(7):513–9.

Sarafianos SG, Das K, Clark Jr AD, Ding J, Boyer PL, Hughes SH, et al. Lamivudine (3TC) resistance in HIV-1 reverse transcriptase involves steric hindrance with beta-branched amino acids. Proc Natl Acad Sci USA 1999;96(18):10027–32.

Selmi B, Boretto J, Sarfati SR, Guerreiro C, Canard B. Mechanism-based suppression of dideoxynucleotide resistance by K65R human

immunodeficiency virus reverse transcriptase using an alpha-boranophosphate nucleoside analogue. J Biol Chem 2001;276(51): 48466–72.
Shirasaka T, Kavlick MF, Ueno T, Gao WY, Kojima E, Alcaide ML, et al. Emergence of human immunodeficiency virus type 1 variants with resistance to multiple dideoxynucleosides in patients receiving therapy with dideoxynucleosides. Proc Natl Acad Sci USA 1995;92(6):2398–402.
Srinivas RV, Fridland A. Antiviral activities of 9-*R*-2-phosphonomethoxypropyl adenine (PMPA) and bis(isopropyloxymethylcarbonyl)PMPA against various drug-resistant human immunodeficiency virus strains. Antimicrob Agents Chemother 1998;42(6):1484–7.
Starnes MC, Cheng YC. Cellular metabolism of 2′,3′-dideoxycytidine, a compound active against human immunodeficiency virus in vitro. J Biol Chem 1987;262(3):988–91.
Tuske S, Sarafianos SG, Clark Jr AD, Ding J, Naeger LK, White KL, et al. Structures of HIV-1 RT-DNA complexes before and after incorporation of the anti-AIDS drug tenofovir. Nat Struct Mol Biol 2004;11(5): 469–74.
Wainberg MA, Drosopoulos WC, Salomon H, Hsu M, Borkow G, Parniak M, et al. Enhanced fidelity of 3TC-selected mutant HIV-1 reverse transcriptase. Science 1996;271(5253):1282–5.
Weiner MP, Costa GL, Schoettlin W, Cline J, Mathur E, Bauer JC. Site-directed mutagenesis of double-stranded DNA by the polymerase chain reaction. Gene 1994;151(1–2):119–23.
Winters MA, Coolley KL, Girard YA, Levee DJ, Hamdan H, Shafer RW, et al. A 6-basepair insert in the reverse transcriptase gene of human immunodeficiency virus type 1 confers resistance to multiple nucleoside inhibitors. J Clin Invest 1998;102(10):1769–75.
Yoshimura K, Feldman R, Kodama E, Kavlick MF, Qiu YL, Zemlicka J, et al. In vitro induction of human immunodeficiency virus type 1 variants resistant to phosphoralaninate prodrugs of *Z*-methylenecyclopropane nucleoside analogues. Antimicrob Agents Chemother 1999;43(10):2479–83.

Design of a Novel HIV-1 Fusion Inhibitor That Displays a Minimal Interface for Binding Affinity

Shinya Oishi,*,† Saori Ito,† Hiroki Nishikawa,† Kentaro Watanabe,† Michinori Tanaka,† Hiroaki Ohno,† Kazuki Izumi,‡ Yasuko Sakagami,‡ Eiichi Kodama,‡ Masao Matsuoka,‡ and Nobutaka Fujii*,†

Graduate School of Pharmaceutical Sciences, Kyoto University, Sakyo-ku, Kyoto 606-8501, Japan, and Laboratory of Virus Immunology, Institute for Virus Research, Kyoto University, Sakyo-ku, Kyoto 606-8507, Japan

Received September 6, 2007

Abstract: Reported herein are the design, biological activities, and biophysical properties of a novel HIV-1 membrane fusion inhibitor. α-Helix-inducible X-EE-XX-KK motifs were applied to design an enfuvirtide analogue **2** that exhibited highly potent anti-HIV activity against wild-type HIV-1, enfuvirtide-resistant HIV-1 strains, and an HIV-2 strain in vitro. Indispensable residues for bioactivity of enfuvirtide, including the residues interacting with the N-terminal heptad repeat and the C-terminal hydrophobic residues, were identified.

The viral entry process of human immunodeficiency virus type 1 (HIV-1[a]) into target cells is mediated by envelope glycoprotein gp41. Formation of a fusogenic six-helical bundle structure consisting of a gp41 N-terminal heptad repeat (NHR) and C-terminal heptad repeat (CHR) promotes the fusion of viral and cellular membranes (Figure 1a).[1] Enfuvirtide **1** (T-20, DP178) is an approved anti-HIV peptide derived from the gp41 CHR.[2,3] This first drug that inhibits HIV-1 entry into the cell is utilized as an alternative anti-HIV agent for patients with drug resistance to reverse transcriptase and/or protease inhibitors. It is believed that peptide **1** interacts with the NHR of gp41 prehairpin structure[4] and associates with the cell or viral membrane through a C-terminal tryptophan-rich region,[5–7] but the exact action mechanism of **1** has not been clarified.[8,9]

Stabilization of bioactive conformations of peptides is a promising approach to enhance their biological potency and to understand the bioactive conformation. Several approaches to stabilize the α-helix structure of gp41 CHR have been reported including macrocyclization by covalent bond formation[10] or salt-bridge formation[11–13] between two adjacent residues and/or introduction of α-helix-inducible peptide sequences.[11] The analogue of another CHR peptide C34, in which the residues on the outer surface of the six-helical bundle were comprehensively replaced with glutamates (Glu) or lysines (Lys), retained highly potent anti-HIV activity.[12] This indicates that the substituted residues are not associated with an NHR coiled-coil as suggested by the crystal structure of the N36-C34 complex.[14] Our expectation was that the following three functional surfaces of **1** could be characterized by extending this molecular design (Figure 1b): (1) minimal interface residues for affinity with NHR; (2) solvent-accessible sites to be utilized for α-helix inducible salt bridges; (3) another functional region outside the α-helix structure. Accordingly, efforts herein were undertaken to design novel amphiphilic enfuvirtide derivatives bearing α-helix-inducible motifs.

A schematic wheel of the potential α-helix structure of peptide **1** is depicted in Figure 1c. To introduce salt bridges between *i* and *i* + 4 residues on the basis of the previous C34 modification,[12] Glu and Lys were arranged at b/c and f/g positions, respectively, so that four consecutive X-EE-XX-KK motifs appeared in the designed peptide **2** (designated T-20EK, Figure 2). All peptides were prepared by standard Fmoc-based peptide synthesis protocol. After final deprotection and cleavage from the resins using a TFA/thioanisole/*m*-cresol/ethanedithiol/H_2O (80:5:5:5:5) cocktail, the crude peptides were purified by reverse-phase HPLC to yield the expected peptides, which were characterized by mass spectrometry. Anti-HIV activity of the peptides against laboratory HIV-1 NL4-3 strain (wild-type) was evaluated by MAGI assay (Table 1). Peptide **2** exhibited 8-fold greater anti-HIV activity compared with the parent peptide **1** [peptide **1**, EC_{50} = 15 ± 3.9 nM; peptide **2**, EC_{50} = 1.8 ± 0.4 nM].[15] The circular dichroism (CD) spectrum of **2** in phosphate buffered saline (pH 7.4) had negative minima at 208 and 222 nm, indicating the presence of an α-helical conformation, while that of **1** suggested a random-coil conformation (Figure 3a). The significant increase in anti-HIV activity of **2** could be rationalized by the preordered stable α-helical structure upstream of L158.[16]

Systematic substitutions of the amino acids at the b, c, f, and g positions with Glu or Lys were extended (Figure 2). Peptide **3**, in which L130 and N160 were substituted with Lys and Glu, respectively, showed anti-HIV activity similar to that of peptide **2** (peptide **3**, EC_{50} = 2.8 ± 0.6 nM). This is consistent with the fact that potent T-1249 also contains these two substitutions.[17] Further replacement toward the N-terminal f position (S129) was again permissive of the high anti-HIV activity (peptide **4**, EC_{50} = 2.5 ± 0.6 nM). On the other hand, replacement of W161 with Glu resulted in a significant decrease of anti-HIV activity as observed in peptides **5** and **6** (EC_{50} = 185 and 111 nM, respectively), indicating that W161 may be located outside the amphiphilic α-helical region. This result correlates with the reduced entry ability of W161F mutant virus.[18] Alanine substitution of W161 also supports the relevance of this residue in virus infectivity and in the inhibitory activity of **1**. Although peptide **7**, carrying a W155A substitution, expressed anti-HIV activity similar to that of peptide **2** (peptide **7**, EC_{50} = 5.8 ± 1.0 nM), W159A, W161A, and F162A substitutions showed reduced bioactivity (peptides **8**, **9**, and **10**, EC_{50} = 49, 24, and 27 nM, respectively). The observed similar CD spectra among peptides **2** and **7**–**10** demonstrated that alanine substitution had no effect on the stabilized secondary structure of the α-helix (Figure 3b). That is, the hydrophobic indole and phenyl groups of these peptides may contribute to their direct interaction with virus components such as gp41 NHR or the virus membrane.[19]

The comparative binding affinity of peptides **1** and **2** with the gp41 NHR sequence was investigated by pull-down assay using synthetic His-tagged CHR peptides and recombinant MBP-fused NHR protein (Figure 4a). Peptide **2** showed higher affinity with NHR compared with **1**. In contrast, only weak binding was observed in the same experiment using all-D-T-20EK D-**2**, which consists of all D-amino acids, indicating that

* To whom correspondence should be addressed. Phone: +81-75-753-4551. Fax: +81-75-753-4570. E-mail: for S.O., soishi@pharm.kyoto-u.ac.jp; for N.F., nfujii@pharm.kyoto-u.ac.jp.

† Graduate School of Pharmaceutical Sciences.

‡ Institute for Virus Research.

[a] Abbreviations: HIV-1, human immunodeficiency virus type 1; NHR, N-terminal heptad repeat; CHR, C-terminal heptad repeat.

10.1021/jm701109d CCC: $40.75
Published on Web 01/16/2008

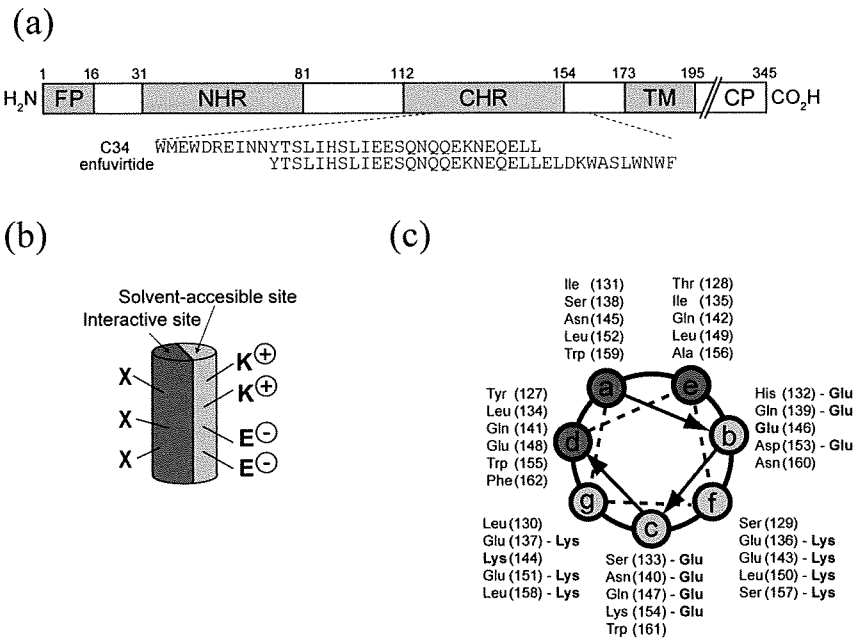

Figure 1. Design of enfuvirtide analogues: (a) schematic representation of HIV-1 gp41 (FP, fusion peptide; NHR, N-terminal heptad repeat; CHR, C-terminal heptad repeat; TM, transmembrane domain); (b) estimated preordered α-helix structure of CHR peptide by potential salt-bridge formation; (c) helical-wheel representation of peptides **1** and **2**. For peptide **2**, Glu residues are in b and c positions and Lys residues in f and g positions. Residues are numbered starting at the first amino acid of the NL4-3 gp41.

Ac-YTSLIHSLIEESQNQQEKNEQELLELDKWASLWNWF-$CONH_2$	**1** (enfuvirtide)
Ac------**EE**--**KK**-**EE**--K---**E**--**KK**-**EE**--**KK**-----$CONH_2$	**2**
Ac----K-**EE**--**KK**-**EE**--K---**E**--**KK**-**EE**--**KK**-E---$CONH_2$	**3**
Ac---KK-**EE**--**KK**-**EE**--K---**E**--**KK**-**EE**--**KK**-E---$CONH_2$	**4**
Ac----K-**EE**--**KK**-**EE**--K---**E**--**KK**-**EE**--**KK**-EE--$CONH_2$	**5**
Ac---KK-**EE**--**KK**-**EE**--K---**E**--**KK**-**EE**--**KK**-EE--$CONH_2$	**6**
Ac------**EE**--**KK**-**EE**--K---**E**--**KK**-**EE**A-**KK**-----$CONH_2$	**7**
Ac------**EE**--**KK**-**EE**--K---**E**--**KK**-**EE**--**KK**A----$CONH_2$	**8**
Ac------**EE**--**KK**-**EE**--K---**E**--**KK**-**EE**--**KK**--A--$CONH_2$	**9**
Ac------**EE**--**KK**-**EE**--K---**E**--**KK**-**EE**--**KK**---A-$CONH_2$	**10**
Ac-LDAN-TK-L--A-I-----MY--QK-NQ-DIFS----$CONH_2$	**11**
Ac-WQEWEQK-TA-L-QA-I------Y--QK--------E---$CONH_2$	T-1249

Figure 2. Peptide sequences of enfuvirtide, enfuvirtide analogues, and T-1249.

Table 1. Anti-HIV Activity of Synthetic Enfuvirtide Analogues

peptide	EC_{50} (nM)[a]	peptide	EC_{50} (nM)[a]
1 (enfuvirtide)	15 ± 3.9	**7**	5.8 ± 1.0
2[b]	1.8 ± 0.4	**8**	49 ± 8.6
3	2.8 ± 0.6	**9**	24 ± 3.8
4	2.5 ± 0.6	**10**	27 ± 6.8
5	185 ± 17	C34	4.5 ± 0.5
6	111 ± 25		

[a] EC_{50} was determined as the concentration that blocked HIV-1 replication by 50% in MAGI assay. [b] The enantiomer of peptide **2** (D-**2**) did not show anti-HIV activity at 10 μM.

the binding between **2** and NHR is specific. In addition, peptide **2** inhibited the interaction between **1** and NHR in lower concentration in the inhibition experiment (Figure 4b).[20]

We next evaluated the anti-HIV activity of peptide **2** against enfuvirtide-resistant variants HIV-1_{V38A} and HIV-1_{N43D}, which were mainly isolated from patients resistant to enfuvirtide (Table 2).[21] Because of the deficient replication of these variants,[22] an additional D36G mutation was experimentally added to these variants and to the wild-type virus. The D36G mutation is not involved in enfuvirtide resistance, but it did improve the sensitivity against **1** [EC_{50}(HIV-1_{D36G}) = 2.3 nM] compared with wild-type HIV-1. As reported previously,[21] V38A and N43D mutations significantly reduced the potency of **1** [EC_{50} (HIV-1_{V38A}) = 22 nM; EC_{50}(HIV-1_{N43D}) = 46 nM]. On the other hand, peptide **2** retained similar anti-HIV activity against N43D and slightly less potent activity toward V38A variants [EC_{50}(HIV-1_{V38A}) = 3.3 nM; EC_{50}(HIV-1_{N43D}) = 1.7 nM]. It is of interest that the anti-HIV activity was restored by induction of a bioactive α-helix structure using X-EE-XX-KK motifs on a CHR peptide. This implies that the stable α-helical structure of **2** can overcome the reduced affinity derived from the mismatched interaction between mutated NHR sequences and peptide **1**.

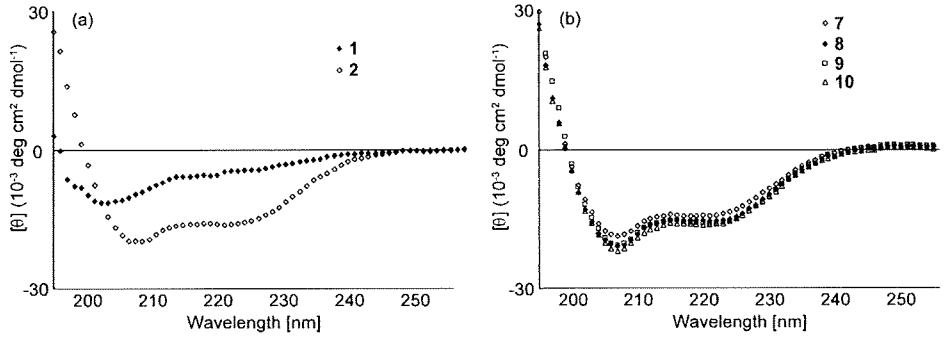

Figure 3. Circular dichroism spectra of (a) peptides **1** and **2** and (b) Ala-substituted peptides **7**–**10**.

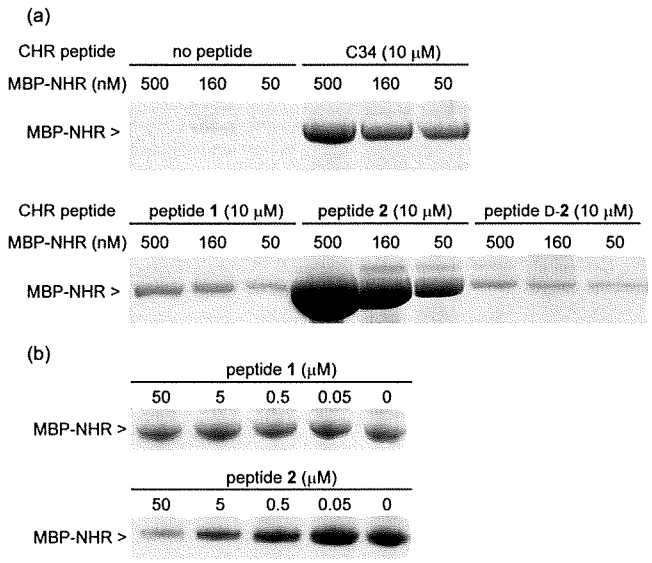

Figure 4. Interaction of His-tagged CHR peptides with MBP-NHR protein by pull-down assay and SDS−PAGE: (a) NHR protein binding with several His-tagged CHR peptides; (b) inhibition of interaction between His-tagged enfuvirtide and NHR protein by nontagged peptides **1** and **2**.

Table 2. Anti-HIV Activity of Peptides **1** and **2** against Enfuvirtide-Resistant Variant and HIV-2 Strains

	EC_{50} (nM)[a]	
strains	peptide **1**	peptide **2**
HIV-1		
NL4–3	15 ± 3.9	1.8 ± 0.4
D36G	2.3 ± 0.5	0.9 ± 0.2
D36G V38A	22 ± 7.6	3.3 ± 1.0
D36G N43D	46 ± 9.6	1.7 ± 0.3
HIV-2		
EHO[b]	37 ± 10	1.5 ± 0.5

[a] EC_{50} was determined as the concentration that blocked HIV-1 replication by 50% in MAGI assay. [b] The antiviral activity (EC_{50}) of peptide **11** against EHO strain was 2.1 ± 0.7 nM.

Interestingly, peptide **2** showed potent antiviral activity even against an HIV-2 EHO strain [EC_{50} = 1.5 nM], which is as potent as peptide **11** having a congenerous sequence derived from the EHO strain [EC_{50} = 2.1 nM].[23] This is in contrast to the previous report on the reduced activity of **1** against the EHO strain [EC_{50} = 37 nM].[24] The potent bioactivity of **2** can be rationalized by the minimal difference of the interface residues between HIV-1 and -2 and the stabilized α-helix structure. Among 19 different residues between the sequences of NL4-3 and EHO strains, 13 residues are located at the solvent accessible sites (b, c, f, and g positions). Although the other six residues are possibly involved in the direct interaction, the potential reduced interactions derived from the mismatch could be recovered by introduction of X-EE-XX-KK motifs.

In conclusion, remodeling of **1** to yield the preordered α-helical structure of **2** led to improved affinity with NHR and increased antiviral activity even against enfuvirtide-resistant HIV-1 and HIV-2 strains. This approach also helped to clarify the potential minimal interface of **1** with viral gp41. Peptide **2** could be a useful chemical tool to understand the membrane fusion process of HIV-1 and the detailed action mechanism of enfuvirtide.

Acknowledgment. This work was supported by a Grant-in-Aid for Scientific Research from the Ministry of Education, Culture, Sports, Science, and Technology of Japan, Health and Labour Sciences Research Grants (Research on HIV/AIDS), the 21st Century COE Program's "Knowledge Information Infrastructure for Genome Science", and the Japan Science and Technology Agency. H.N. is grateful for the JSPS Research Fellowships for Young Scientists. Appreciation is expressed to Dr. Masaru Hoshino (Kyoto University) for helpful discussions and to Mr. Maxwell Reback (Kyoto University) for reading the manuscript.

Supporting Information Available: Experimental details for peptide preparation, CD spectra measurements, and bioassays and MS and HPLC data. This material is available free of charge via the Internet at http://pubs.acs.org.

References

(1) Lu, M.; Blacklow, S. C.; Kim, P. S. A trimeric structural domain of the HIV-1 transmembrane glycoprotein. *Nat. Struct. Biol.* **1995**, *2*, 1075–1082.
(2) Wild, C. T.; Shugars, D. C.; Greenwell, T. K.; McDanal, C. B.; Matthews, T. J. Peptides corresponding to a predictive alpha-helical domain of human immunodeficiency virus type 1 gp41 are potent inhibitors of virus infection. *Proc. Natl. Acad. Sci. U.S.A.* **1994**, *91*, 9770–9774.
(3) Matthews, T.; Salgo, M.; Greenberg, M.; Chung, J.; DeMasi, R.; Bolognesi, D. Enfuvirtide: the first therapy to inhibit the entry of HIV-1 into host CD4 lymphocytes. *Nat. Rev. Drug. Discovery* **2004**, *3*, 215–225.
(4) Lawless, M. K.; Barney, S.; Guthrie, K. I.; Bucy, T. B.; Petteway, S. R., Jr.; Merutka, G. HIV-1 membrane fusion mechanism: structural studies of the interactions between biologically-active peptides from gp41. *Biochemistry* **1996**, *35*, 13697–13708.
(5) Kliger, Y.; Gallo, S. A.; Peisajovich, S. G.; Munoz-Barroso, I.; Avkin, S.; Blumenthal, R.; Shai, Y. Mode of action of an antiviral peptide from HIV-1. Inhibition at a post-lipid mixing stage. *J. Biol. Chem.* **2001**, *276*, 1391–1397.
(6) Cardoso, R. M.; Zwick, M. B.; Stanfield, R. L.; Kunert, R.; Binley, J. M.; Katinger, H.; Burton, D. R.; Wilson, I. A. Broadly neutralizing anti-HIV antibody 4E10 recognizes a helical conformation of a highly conserved fusion-associated motif in gp41. *Immunity* **2005**, *22*, 163–173.
(7) Wexler-Cohen, Y.; Johnson, B. T.; Puri, A.; Blumenthal, R.; Shai, Y. Structurally altered peptides reveal an important role for N-terminal heptad repeat binding and stability in the inhibitory action of HIV-1 peptide DP178. *J. Biol. Chem.* **2006**, *281*, 9005–9010.
(8) Liu, S.; Lu, H.; Niu, J.; Xu, Y.; Wu, S.; Jiang, S. Different from the HIV fusion inhibitor C34, the anti-HIV drug Fuzeon (T-20) inhibits HIV-1 entry by targeting multiple sites in gp41 and gp120. *J. Biol. Chem.* **2005**, *280*, 11259–11273.
(9) Liu, S.; Jing, W.; Cheung, B.; Lu, H.; Sun, J.; Yan, X.; Niu, J.; Farmar, J.; Wu, S.; Jiang, S. HIV gp41 C-terminal heptad repeat contains multifunctional domains. Relation to mechanisms of action of anti-HIV peptides. *J. Biol. Chem.* **2007**, *282*, 9612–9620.
(10) Judice, J. K.; Tom, J. Y.; Huang, W.; Wrin, T.; Vennari, J.; Petropoulos, C. J.; McDowell, R. S. Inhibition of HIV type 1 infectivity by constrained α-helical peptides: implications for the viral fusion mechanism. *Proc. Natl. Acad. Sci. U.S.A.* **1997**, *94*, 13426–13430.
(11) Joyce, J. G.; Hurni, W. M.; Bogusky, M. J.; Garsky, V. M.; Liang, X.; Citron, M. P.; Danzeisen, R. C.; Miller, M. D.; Shiver, J. W.; Keller, P. M. Enhancement of α-helicity in the HIV-1 inhibitory peptide DP178 leads to an increased affinity for human monoclonal antibody 2F5 but does not elicit neutralizing responses in vitro. *J. Biol. Chem.* **2002**, *277*, 45811–45820.
(12) Otaka, A.; Nakamura, M.; Nameki, D.; Kodama, E.; Uchiyama, S.; Nakamura, S.; Nakano, H.; Tamamura, H.; Kobayashi, Y.; Matsuoka, M.; Fujii, N. Remodeling of gp41-C34 peptide leads to highly effective inhibitors of the fusion of HIV-1 with target cells. *Angew. Chem., Int. Ed.* **2002**, *41*, 2937–2940.
(13) Dwyer, J. J.; Wilson, K. L.; Davison, D. K.; Freel, S. A.; Seedorff, J. E.; Wring, S. A.; Tvermoes, N. A.; Matthews, T. J.; Greenberg, M. L.; Delmedico, M. K. Design of helical, oligomeric HIV-1 fusion inhibitor peptides with potent activity against enfuvirtide-resistant virus. *Proc. Natl. Acad. Sci. U.S.A.* **2007**, *104*, 12772–12777.
(14) Chan, D. C.; Fass, D.; Berger, J. M.; Kim, P. S. Core structure of gp41 from the HIV envelope glycoprotein. *Cell* **1997**, *89*, 263–273.
(15) Cytotoxicity of peptide **2** was not observed even at 10 μM.
(16) Additional effects on increasing the anti-HIV activity such as formation of intra- and intermolecular salt bridges are also possible.
(17) Eron, J. J.; Gulick, R. M.; Bartlett, J. A.; Merigan, T.; Arduino, R.; Kilby, J. M.; Yangco, B.; Diers, A.; Drobnes, C.; DeMasi, R.;

Greenberg, M.; Melby, T.; Raskino, C.; Rusnak, P.; Zhang, Y.; Spence, R.; Miralles, G. D. Short-term safety and antiretroviral activity of T-1249, a second-generation fusion inhibitor of HIV. *J. Infect. Dis.* **2004**, *189*, 1075–1083.

(18) Salzwedel, K.; West, J. T.; Hunter, E. A conserved tryptophan-rich motif in the membrane-proximal region of the human immunodeficiency virus type 1 gp41 ectodomain is important for Env-mediated fusion and virus infectivity. *J. Virol.* **1999**, *73*, 2469–2480.

(19) Wexler-Cohen, Y.; Johnson, B. T.; Puri, A.; Blumenthal, R.; Shai, Y. Structurally altered peptides reveal an important role for N-terminal heptad repeat binding and stability in the inhibitory action of HIV-1 peptide DP178. *J. Biol. Chem.* **2006**, *281*, 9005–9010.

(20) Since a large excess of CHR peptides to NHR protein was utilized for the pull-down assay, the inhibitory concentration in this experiment was less than that observed in the MAGI assay. It is conceivable that the anti-HIV activity in the MAGI assay might be observed with less fully occupied one or two CHR peptides bound per NHR trimer.

(21) Cabrera, C.; Marfil, S.; Garcia, E.; Martinez-Picado, J.; Bonjoch, A.; Bofill, M.; Moreno, S.; Ribera, E.; Domingo, P.; Clotet, B.; Ruiz, L. Genetic evolution of gp41 reveals a highly exclusive relationship between codons 36, 38 and 43 in gp41 under long-term enfuvirtide-containing salvage regimen. *AIDS* **2006**, *20*, 2075–2080.

(22) Mink, M.; Mosier, S. M.; Janumpalli, S.; Davison, D.; Jin, L.; Melby, T.; Sista, P.; Erickson, J.; Lambert, D.; Stanfield-Oakley, S. A.; Salgo, M.; Cammack, N.; Matthews, T.; Greenberg, M. L. Impact of human immunodeficiency virus type 1 gp41 amino acid substitutions selected during enfuvirtide treatment on gp41 binding and antiviral potency of enfuvirtide in vitro. *J. Virol.* **2005**, *79*, 12447–12454.

(23) Gustchina, E.; Hummer, G.; Bewley, C. A.; Clore, G. M. Differential inhibition of HIV-1 and SIV envelope-mediated cell fusion by C34 peptides derived from the C-terminal heptad repeat of gp41 from diverse strains of HIV-1, HIV-2, and SIV. *J. Med. Chem.* **2005**, *48*, 3036–3044.

(24) Witvrouw, M.; Pannecouque, C.; Switzer, W. M.; Folks, T. M.; De Clercq, E.; Heneine, W. Susceptibility of HIV-2, SIV and SHIV to various anti-HIV-1 compounds: implications for treatment and post-texposure prophylaxis. *Antiviral Ther.* **2004**, *9*, 57–65.

JM701109D

JOURNAL OF CLINICAL MICROBIOLOGY, Feb. 2008, p. 792–795 Vol. 46, No. 2
0095-1137/08/$08.00+0 doi:10.1128/JCM.01470-07

Dual-Reporter Phenotypic Assay for Human Immunodeficiency Viruses[▽]

Keiko Kajiwara, Eiichi Kodama,* Yasuko Sakagami, Takeshi Naito, and Masao Matsuoka

Laboratory of Virus Immunology, Institute for Virus Research, Kyoto University, 53 Kawaramachi, Shogoin, Sakyo-ku, Kyoto 606-8507, Japan

Received 22 July 2007/Returned for modification 27 September 2007/Accepted 5 December 2007

We have established a novel human immunodeficiency virus (HIV) tandem-reporter assay using HIV receptor-transduced NP-2 cells with long terminal repeat-controlled β-galactosidase, inserted internal ribosome entry site, and secretary alkaline phosphatase genes. This assay allows users to detect replication of clinical isolates, indicating its useful application as an HIV phenotypic assay.

Assays for detecting the emergence of resistant variants, as well as evaluating clinical efficacy, provide useful information regarding chemotherapy for human immunodeficiency virus (HIV) infection. To date, two types of assay systems have been developed and approved, namely, genotypic and phenotypic assays (13, 31). Genotypic assays detect genetic mutations that are associated with drug resistance and lead to rapid and sensitive detection of the emergence of resistant variants (9), although they only provide estimated resistance profiles (16, 30). Lists of significant resistance-associated mutations in reverse transcriptase (RT), protease, and envelope genes are maintained by some organizations and Universities, such as the International AIDS Society-USA (http://iasusa.org/resistance mutations); Los Alamos National Laboratory, Los Alamos, NM (http://resdb.lanl.gov/Resist_DB); and the Stanford University, Stanford, CA (http://hivdb.stanford.edu/index.html). PCR-based genotypic assays are heavily dependent on the primers used. Therefore, some biases must unfortunately be presumed, since most primer-matched sequences are preferentially amplified, resulting in some discordance with phenotypic assays (21, 33) that are time-consuming and require tedious procedures because isolation of replication-competent viruses is required. To date, phenotypic assays for clinical isolates have been mainly performed in experiments with a p24 production assay in phytohemagglutinin-stimulated peripheral blood mononuclear cells (27, 32, 34).

For more rapid and simple phenotypic assays, recombinant viruses containing the region responsible for resistance have been utilized instead of isolated viruses (14, 18, 35). However, since protease resistance mutations are introduced simultaneously with gag mutations (4, 25), cloning of the entire gag and protease coding region is occasionally required. Recently, mutations for 3′-azido-3′-deoxythymidine (AZT) resistance have been identified in the connection and/or RNase H subdomain (5, 7, 26), which no commercially available genotypic and phenotypic assays include for the analysis. Moreover, the mechanism of resistance to a fusion inhibitor, enfuvirtide, is a complex issue, since mutations in not only the gp41 coding region (6, 24) but also the V3 region (29) and the CD4-binding site (2) of gp120 influence the susceptibility, indicating that patient-derived viruses are ideally required for evaluation of drug susceptibility.

Recently, Hachiya et al. established a simple and rapid phenotypic assay using MAGIC5 cells (CCR5-transduced MAGI cells) (11). This system efficiently isolates clinical HIV variants and has proven to be useful for evaluating drug susceptibility (12). However, the expression of transduced receptors on MAGIC5 cells declines during prolonged culture, as described for MAGI cells (17). Therefore, in order to obtain HIV isolates efficiently and perform the assay, relatively fresh cells are required. More recently, we established a tetrazolium-based colorimetric assay for monitoring replications of not only CXCR4 (X4)-tropic but also CCR5 (R5)-tropic HIVs and drug susceptibilities (17). We reported that NCK45 cells stably express HIV receptors on their cell surface and provide reproducible results (17). Since this assay depends on the cytopathic effect induced by HIV, it appears to be insufficient for assessing infections with no or a few cytopathic variants. Furthermore, it requires 7 days of culture to obtain the drug susceptibility. In the present study, we have established a novel single long terminal repeat (LTR)-driven tandem two-reporter system using the internal ribosome entry site (IRES) (15), which enables the evaluation of drug susceptibility within 2 days for various HIVs, including clinical isolates.

To construct an LTR-driven reporter vector, an amplified LTR region (the −138 to +89 region of the transcriptional start site of HIV-1 molecular clone pNL4-3) was inserted into pβgal-Basic (Clontech Laboratories, Inc., Palo Alto, CA) between the NheI and HindIII sites (pLTR-βgal). The 5′ region (HindIII to EcoRV) of the β-galactosidase gene was replaced with the responsible β-galactosidase fragment with nuclear localization signal sequence (MPKKKRK) amplified from genomic DNA of MAGI cells (20). Fragments of IRES and secretory alkaline phosphatase (SEAP) were amplified from pIRES2-EGFP and pSEAP2-Basic (Clontech Laboratories, Inc.), respectively. A puromycin-resistance gene (Puro^r) under the control of the phosphoglycerate kinase promoter as a selection marker was inserted at the SalI site of the vector (pLTR-β-Gal/SEAP-Puro^r), as shown in Fig. 1A. All fragments were verified by sequencing.

The pLTR-β-Gal/SEAP-Puro^r plasmid was transfected into NCK45 cells (CD4, CXCR4, and CCR5-transduced NP-2 cells

* Corresponding author. Mailing address: Laboratory of Virus Immunology, Institute for Virus Research, Kyoto University, 53 Kawaramachi, Shogoin, Sakyo-ku, Kyoto 606-8507, Japan. Phone and fax: 81-75-751-3986. E-mail: ekodama@virus.kyoto-u.ac.jp.

▽ Published ahead of print on 19 December 2007.

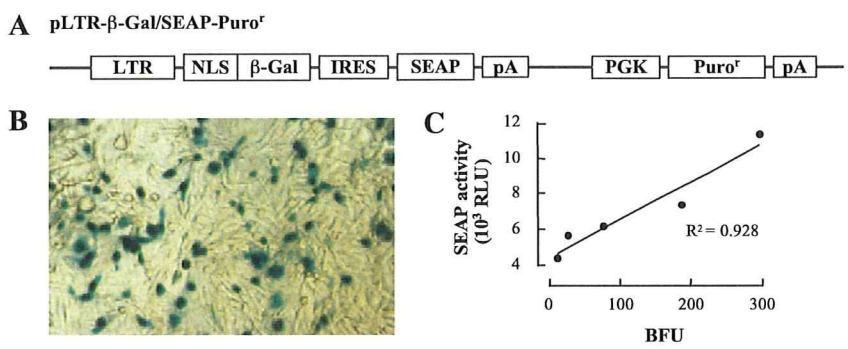

FIG. 1. Establishment of a cell line with β-galactosidase (β-Gal) and SEAP genes driven by an LTR. (A) Schematic diagram of the vector used in the present study, which simultaneously expresses genes for β-Gal and SEAP under the control of the HIV-1 LTR promoter (pLTR-β-Gal/SEAP-Puro^r). The enhancer region (positions −138 to +89) of the LTR, the nuclear localization signal (NLS) derived from the T-antigen of simian virus 40, the IRES, the phosphoglycerate kinase promoter (PGK), and the polyadenylation signal (pA) are also shown. (B) Microscopic image of X-Gal-stained NCK45-β-Gal/SEAP cells at 48 h after virus inoculation. (C) Correlation between β-Gal and SEAP activities in culture supernatants. NCK45-β-Gal/SEAP cells were infected with HIV at various infectious doses and incubated for 48 h. Culture supernatants were examined for their SEAP activities and expressed as relative right units (RLU). BFU, blue-cell-forming units.

derived from a glioma) (17, 36) to detect intracellular Tat expression through the LTR-driven tandem reporter genes. At 48 h after transfection, the cells were cultured in Dulbecco modified Eagle medium (Sigma, St. Louis, MO) supplemented with 5% heat-inactivated fetal calf serum, 0.5 mg of G418 disulfate (Nacalai Tesque, Kyoto, Japan)/ml, 0.2 mg of hygromycin B (Calbiochem, La Jolla, CA)/ml, and 10 μg of puromycin (Sigma)/ml and designated NCK45-β-Gal/SEAP cells. The expression levels of receptors on NCK45 cells confirmed by a flow cytometer (17) were 97, 83, and 99%, while those on H9 cells as a control were 65, 73, and 0.3% for CD4, CXCR4, and CCR5, respectively.

To evaluate anti-HIV agents, NCK45-β-Gal/SEAP cells (5×10^4 cells/ml) in Dulbecco modified Eagle medium-based culture medium supplemented with 5% fetal calf serum, penicillin, and streptomycin were seeded onto 96-well plates. On the following day, the cells were inoculated with sample viruses at 60 blue-cell-forming units (BFU)/well, incubated for 48 h, and then cultured in the presence of various concentrations of drugs. After 48 h of culture, the cells were fixed with 1% formaldehyde and 0.2% glutaraldehyde for 3 min, washed three times with phosphate-buffered saline, and incubated with X-Gal (5-bromo-4-chloro-3-indolyl-β-D-galactopyranoside) for 2 h (Fig. 1B). To evaluate the SEAP activities, the culture supernatants were harvested and analyzed by using a Great EscAPe SEAP chemiluminescent detection kit (BD Biosciences Clontech, Palo Alto, CA) according to the manufacturer's protocol. Samples were measured by using a Wallac 1450 MicroBeta Jet Luminometer (Perkin-Elmer, Wellesley, MA). For comparison, MAGI-CCR5 cells were analyzed as previously described (17).

The activities of various anti-HIV agents toward NCK45-β-Gal/SEAP cells were compared to those in the MAGI assay. The BFU and SEAP activities were well correlated with the viral input (Fig. 1C; correlation coefficient $R^2 = 0.928$). We tested various anti-HIV agents (Table 1): DS5000, an adsorption inhibitor; AZT and 2′,3′-dideoxycytidine (ddC), RT inhibitors; T-140 (37), a CXCR4 antagonist; and TAK-779, a CCR5 antagonist (1). The antiviral activities of the compounds determined by each reporter in NCK45-β-Gal/SEAP cells were comparable to those obtained using MAGI cells, although some were statistically significant (Table 1). Intracellular nucleoside/nucleotide metabolisms, especially thymidine kinase (10), and expression levels of receptors (19) may alter the 50% effective concentrations of the AZT and CCR5 antagonists, respectively.

NCK45-β-Gal/SEAP cells also supported the replication of various clinical isolates, as well as laboratory strains. The clin-

TABLE 1. Comparison of anti-HIV activities in MAGI and NCK45-β-Gal/SEAP cells

Compound	Target	Mean EC_{50} (μM)[a] ± SD						CC_{50} (μM)[b] (NCK45-β-Gal/SEAP)
		HIV-1_{IIIB}			HIV-1_{Ba-L}			
		MAGI	NCK45-β-Gal/SEAP		MAGI	NCK45-β-Gal/SEAP		
			β-Gal	SEAP		β-Gal	SEAP	
DS5000	gp120	0.14 ± 0.025	0.076 ± 0.026	0.07 ± 0.0034	0.36 ± 0.052	0.49 ± 0.069	0.42 ± 0.15	>100
AZT	RT	0.031 ± 0.013*	0.0043 ± 0.0022	0.0035 ± 0.0007	0.05 ± 0.029	0.0035 ± 0.0007	0.0094 ± 0.0063	>100
ddC	RT	0.4 ± 0.16	0.53 ± 0.12	0.42 ± 0.14	0.48 ± 0.17	0.72 ± 0.067	0.67 ± 0.2	>100
T-140	CXCR4	0.006 ± 0.0006	0.006 ± 0.0002	0.0025 ± 0.0008	>100	>100	>100	>100
TAK-779	CCR5	>100	>100	>100	0.003 ± 0.0019*	0.035 ± 0.0088	0.027 ± 0.0098	>100

[a] EC_{50}, 50% effective concentration. Data represent mean values of at least three independent experiments. HIV-1_{IIIB} and HIV-1_{Ba-L} utilize CXCR4 (X4) and CCR5 (R5) as coreceptors, respectively. *, The EC_{50} values obtained from MAGI and NCK cells (both β-galactosidase and SEAP) were statistically significant (Student t test, $P < 0.01$).

[b] CC_{50}, 50% cytotoxic concentration. The CC_{50} was determined by the MTT method after 2 days exposure of compounds as described previously (11).

TABLE 2. Drug susceptibility against HIV clinical isolates in MAGI and NCK45-β-Gal/SEAP cells

Compound	Cell line	Detection	EC_{50} (μM)[a]					
			KMT/R5X4	IVR405/R5X4	IVR406/R5X4	IVR409/R5X4	IVR416/R5X4	IVR417/R5
DS5000	MAGI	β-Gal	0.54	0.43	0.18	0.51	0.16	1.4
	NCK45-β-Gal/SEAP	β-Gal	0.6	0.22	0.14	0.46	0.22	1.9
		SEAP	0.28	0.27	0.19	0.28	0.16	1.5
AZT	MAGI	β-Gal	0.0027	>1.0	0.68	0.055	0.046	0.0033
	NCK45-β-Gal/SEAP	β-Gal	0.0038	>1.0	1.0	0.061	0.018	0.004
		SEAP	0.0044	>1.0	0.41	0.032	0.013	0.0015
ddC	MAGI	β-Gal	1.3	0.55	1.4	1.2	1.0	1.3
	NCK45-β-Gal/SEAP	β-Gal	1.0	0.32	1.0	1.3	0.75	0.79
		SEAP	2.0	0.24	2.1	1.5	0.52	0.77

[a] EC_{50}, 50% antiviral effective concentration. Amino acid substitutions in the RT region were as follows: none for KMT, M41L/E44D/D67G/V118I/Q151M/L210W/T215Y for IVR405, M41L/E44D/D67N/V118I/M184I/L210W/T215Y for IVR406, M41L/E44D/M184V/L210W/T215Y for IVR416, and D67N/V106AV/M184V/T215F for IVR407. Coreceptor usage is indicated in each subheading after the slash: R5X4, CCR5 and CXCR4 dualtropic virus; R5, CCR5-tropic virus.

ical isolates used in the present study were kindly provided by Y. Maeda (Kumamoto University School of Medicine, Kumamoto, Japan) and S. Oka (AIDS Clinical Center, International Medical Center of Japan, Tokyo, Japan). The drug susceptibilities of not only R5-tropic isolates but also X4-tropic and dualtropic isolates were comparable to those in the MAGI assay (Table 2). IVR405 and IVR406 were highly resistant to AZT, whereas IVR409 and IVR416 showed moderate resistance to AZT, and KMT and IVR417 were susceptible to AZT. These susceptibilities were confirmed by the MAGI assay.

In the present study, we established an IRES-mediated tandem-reporter assay using NCK45 cells for the rapid and simultaneous evaluation of the antiviral activities of compounds. This assay enables the evaluation of various HIV strains and clinical isolates within 3 days, including the cell preparation procedure. Secreted SEAP from HIV-infected NCK45 cells is also useful for monitoring the isolation of viruses without cell destruction and enables the continuous propagation of the isolates during isolation. Since NCK45-β-Gal/SEAP cells are susceptible to various viruses, including clinical strains, depending on the experimental purpose any HIV variants may be used for a reference virus, e.g., an isolate prior to the therapy. The LTR promoter for the dual reporters used in the present study includes four CpG methylation-sensitive sites, although Tat can transactivate the HIV-1 LTR regardless of the methylation state (3, 28). Thus, reporter genes in NCK45 cells are less affected by gene silencing.

Compared to the commercially available phenotypic assays, our established system may be useful especially for inhibitors targeting new molecules, including envelope proteins and integrase. A fusion inhibitor T-20 can suppress variants refractory to most of approved RT and protease inhibitors (22, 23). Both phenotypic and genotypic assays for T-20 are needed to evaluate the clinical outcome of patients with T-20-containing regimens. An approved CCR5 antagonist, maraviroc, may also suppress such refractory variants (8). Needless to say, to assess the drug susceptibility experimentally and/or clinically, a combination of established databases accumulated with various assays appears to be useful and important.

In conclusion, the tandem reporters β-Gal and SEAP can evaluate the exact viral infectivity and proportional LTR activation level by repetitive analyses of culture supernatants, respectively. This IRES-mediated tandem-reporter system may be applicable to other reporter genes, e.g., the luciferase gene. Thus, our assay system may provide simple, rapid and stable results for HIV phenotypic assays.

We thank J. Overbaugh for providing the HeLa-CD4/CCR5-LTR/β-Gal cells through the AIDS Research and Reference Reagent Program, Division of AIDS, National Institute of Allergy and Infectious Diseases (Bethesda, MD).

This study was supported in part by a grant for the Promotion of AIDS Research from the Ministry of Health and Welfare of Japan (to M.M. and E.K.); a grant for Research for Health Science Focusing on Drug Innovation from the Japan Health Science Foundation (to E.K.); and a grant from the Ministry of Education, Culture, Sports, Science, and Technology of Japan (to E.K.). K.K. and T.N. are supported by the 21st Century COE Program of the Ministry of Education, Culture, Sports, Science, and Technology.

REFERENCES

1. **Baba, M., O. Nishimura, N. Kanzaki, M. Okamoto, H. Sawada, Y. Iizawa, M. Shiraishi, Y. Aramaki, K. Okonogi, Y. Ogawa, K. Meguro, and M. Fujino.** 1999. A small-molecule, nonpeptide CCR5 antagonist with highly potent and selective anti-HIV-1 activity. Proc. Natl. Acad. Sci. USA **96**:5698–5703.
2. **Baldwin, C. E., and B. Berkhout.** 2006. Second site escape of a T20-dependent HIV-1 variant by a single amino acid change in the CD4 binding region of the envelope glycoprotein. Retrovirology **3**:84.
3. **Bednarik, D. P., J. A. Cook, and P. M. Pitha.** 1990. Inactivation of the HIV LTR by DNA CpG methylation: evidence for a role in latency. EMBO J. **9**:1157–1164.
4. **Brann, T. W., R. L. Dewar, M. K. Jiang, A. Shah, K. Nagashima, J. A. Metcalf, J. Falloon, H. C. Lane, and T. Imamichi.** 2006. Functional correlation between a novel amino acid insertion at codon 19 in the protease of human immunodeficiency virus type 1 and polymorphism in the p1/p6 Gag cleavage site in drug resistance and replication fitness. J. Virol. **80**:6136–6145.
5. **Brehm, J. H., D. Koontz, J. D. Meteer, V. Pathak, N. Sluis-Cremer, and J. W. Mellors.** 2007. Selection of mutations in the connection and RNase H domains of human immunodeficiency virus type 1 reverse transcriptase that increase resistance to 3′-azido-3′-dideoxythymidine. J. Virol. **81**:7852–7859.
6. **Cabrera, C., S. Marfil, E. Garcia, J. Martinez-Picado, A. Bonjoch, M. Bofill, S. Moreno, E. Ribera, P. Domingo, B. Clotet, and L. Ruiz.** 2006. Genetic evolution of gp41 reveals a highly exclusive relationship between codons 36, 38, and 43 in gp41 under long-term enfuvirtide-containing salvage regimen. Aids **20**:2075–2080.
7. **Delviks-Frankenberry, K. A., G. N. Nikolenko, R. Barr, and V. K. Pathak.** 2007. Mutations in human immunodeficiency virus type 1 RNase H primer grip enhance 3′-azido-3′-deoxythymidine resistance. J. Virol. **81**:6837–6845.
8. **Fatkenheuer, G., A. L. Pozniak, M. A. Johnson, A. Plettenberg, S. Staszewski, A. I. Hoepelman, M. S. Saag, F. D. Goebel, J. K. Rockstroh, B. J. Dezube, T. M. Jenkins, C. Medhurst, J. F. Sullivan, C. Ridgway, S. Abel, I. T. James, M. Youle, and E. van der Ryst.** 2005. Efficacy of short-term monotherapy

with maraviroc, a new CCR5 antagonist, in patients infected with HIV-1. Nat. Med. **11**:1170–1172.
9. **Frenkel, L. M., L. E. Wagner II, S. M. Atwood, T. J. Cummins, and S. Dewhurst.** 1995. Specific, sensitive, and rapid assay for human immunodeficiency virus type 1 *pol* mutations associated with resistance to zidovudine and didanosine. J. Clin. Microbiol. **33**:342–347.
10. **Gao, W. Y., R. Agbaria, J. S. Driscoll, and H. Mitsuya.** 1994. Divergent anti-human immunodeficiency virus activity and anabolic phosphorylation of 2′,3′-dideoxynucleoside analogs in resting and activated human cells. J. Biol. Chem. **269**:12633–12638.
11. **Hachiya, A., S. Aizawa-Matsuoka, M. Tanaka, Y. Takahashi, S. Ida, H. Gatanaga, Y. Hirabayashi, A. Kojima, M. Tatsumi, and S. Oka.** 2001. Rapid and simple phenotypic assay for drug susceptibility of human immunodeficiency virus type 1 using CCR5-expressing HeLa/CD4$^+$ cell clone 1-10 (MAGIC-5). Antimicrob. Agents Chemother. **45**:495–501.
12. **Hachiya, A., H. Gatanaga, E. Kodama, M. Ikeuchi, M. Matsuoka, S. Harada, H. Mitsuya, S. Kimura, and S. Oka.** 2004. Novel patterns of nevirapine resistance-associated mutations of human immunodeficiency virus type 1 in treatment-naive patients. Virology **327**:215–224.
13. **Hanna, G. J., and R. T. D'Aquila.** 2001. Clinical use of genotypic and phenotypic drug resistance testing to monitor antiretroviral chemotherapy. Clin. Infect. Dis. **32**:774–782.
14. **Hertogs, K., M. P. de Bethune, V. Miller, T. Ivens, P. Schel, A. Van Cauwenberge, C. Van Den Eynde, V. Van Gerwen, H. Azijn, M. Van Houtte, F. Peeters, S. Staszewski, M. Conant, S. Bloor, S. Kemp, B. Larder, and R. Pauwels.** 1998. A rapid method for simultaneous detection of phenotypic resistance to inhibitors of protease and reverse transcriptase in recombinant human immunodeficiency virus type 1 isolates from patients treated with antiretroviral drugs. Antimicrob. Agents Chemother. **42**:269–276.
15. **Jang, S. K., and E. Wimmer.** 1990. Cap-independent translation of encephalomyocarditis virus RNA: structural elements of the internal ribosomal entry site and involvement of a cellular 57-kD RNA-binding protein. Genes Dev. **4**:1560–1572.
16. **Jones, S., and M. E. Klotman.** 2001. Impact of genotypic resistance testing on physician selection of antiretroviral therapy. J. Hum. Virol. **4**:214–216.
17. **Kajiwara, K., E. Kodama, and M. Matsuoka.** 2006. A novel colorimetric assay for CXCR4 and CCR5 tropic human immunodeficiency viruses. Antivir. Chem. Chemother. **17**:215–223.
18. **Kellam, P., and B. A. Larder.** 1994. Recombinant virus assay: a rapid, phenotypic assay for assessment of drug susceptibility of human immunodeficiency virus type 1 isolates. Antimicrob. Agents Chemother. **38**:23–30.
19. **Ketas, T. J., S. E. Kuhmann, A. Palmer, J. Zurita, W. He, S. K. Ahuja, P. J. Klasse, and J. P. Moore.** 2007. Cell surface expression of CCR5 and other host factors influence the inhibition of HIV-1 infection of human lymphocytes by CCR5 ligands. Virology **364**:281–290.
20. **Kimpton, J., and M. Emerman.** 1992. Detection of replication-competent and pseudotyped human immunodeficiency virus with a sensitive cell line on the basis of activation of an integrated β-galactosidase gene. J. Virol. **66**: 2232–2239.
21. **Korn, K., H. Reil, H. Walter, and B. Schmidt.** 2003. Quality control trial for human immunodeficiency virus type 1 drug resistance testing using clinical samples reveals problems with detecting minority species and interpretation of test results. J. Clin. Microbiol. **41**:3559–3565.
22. **Lalezari, J. P., K. Henry, M. O'Hearn, J. S. Montaner, P. J. Piliero, B. Trottier, S. Walmsley, C. Cohen, D. R. Kuritzkes, J. J. Eron, Jr., J. Chung, R. DeMasi, L. Donatacci, C. Drobnes, J. Delehanty, and M. Salgo.** 2003. Enfuvirtide, an HIV-1 fusion inhibitor, for drug-resistant HIV infection in North and South America. N. Engl. J. Med. **348**:2175–2185.
23. **Lazzarin, A., B. Clotet, D. Cooper, J. Reynes, K. Arasteh, M. Nelson, C. Katlama, H. J. Stellbrink, J. F. Delfraissy, J. Lange, L. Huson, R. DeMasi, C. Wat, J. Delehanty, C. Drobnes, and M. Salgo.** 2003. Efficacy of enfuvirtide in patients infected with drug-resistant HIV-1 in Europe and Australia. N. Engl. J. Med. **348**:2186–2195.
24. **Loutfy, M. R., J. M. Raboud, J. S. Montaner, T. Antoniou, B. Wynhoven, F. Smaill, D. Rouleau, J. Gill, W. Schlech, Z. L. Brumme, T. Mo, K. Gough, A. Rachlis, P. R. Harrigan, and S. L. Walmsley.** 2007. Assay of HIV gp41 amino acid sequence to identify baseline variation and mutation development in patients with virologic failure on enfuvirtide. Antivir. Res. **75**:58–63.
25. **Maguire, M. F., R. Guinea, P. Griffin, S. Macmanus, R. C. Elston, J. Wolfram, N. Richards, M. H. Hanlon, D. J. Porter, T. Wrin, N. Parkin, M. Tisdale, E. Furfine, C. Petropoulos, B. W. Snowden, and J. P. Kleim.** 2002. Changes in human immunodeficiency virus type 1 Gag at positions L449 and P453 are linked to I50V protease mutants in vivo and cause reduction of sensitivity to amprenavir and improved viral fitness in vitro. J. Virol. **76**:7398–7406.
26. **Nikolenko, G. N., K. A. Delviks-Frankenberry, S. Palmer, F. Maldarelli, M. J. Fivash, Jr., J. M. Coffin, and V. K. Pathak.** 2007. Mutations in the connection domain of HIV-1 reverse transcriptase increase 3′-azido-3′-deoxythymidine resistance. Proc. Natl. Acad. Sci. USA **104**:317–322.
27. **Perez-Alvarez, L., R. Carmona, A. Ocampo, A. Asorey, C. Miralles, S. Perez de Castro, M. Pinilla, G. Contreras, J. A. Taboada, and R. Najera.** 2006. Long-term monitoring of genotypic and phenotypic resistance to T20 in treated patients infected with HIV-1. J. Med. Virol. **78**:141–147.
28. **Pion, M., A. Jordan, A. Biancotto, F. Dequiedt, F. Gondois-Rey, S. Rondeau, R. Vigne, J. Hejnar, E. Verdin, and I. Hirsch.** 2003. Transcriptional suppression of in vitro-integrated human immunodeficiency virus type 1 does not correlate with proviral DNA methylation. J. Virol. **77**:4025–4032.
29. **Reeves, J. D., S. A. Gallo, N. Ahmad, J. L. Miamidian, P. E. Harvey, M. Sharron, S. Pohlmann, J. N. Sfakianos, C. A. Derdeyn, R. Blumenthal, E. Hunter, and R. W. Doms.** 2002. Sensitivity of HIV-1 to entry inhibitors correlates with envelope/coreceptor affinity, receptor density, and fusion kinetics. Proc. Natl. Acad. Sci. USA **99**:16249–16254.
30. **Rhee, S. Y., J. Taylor, G. Wadhera, A. Ben-Hur, D. L. Brutlag, and R. W. Shafer.** 2006. Genotypic predictors of human immunodeficiency virus type 1 drug resistance. Proc. Natl. Acad. Sci. USA **103**:17355–17360.
31. **Richman, D. D.** 2000. Principles of HIV resistance testing and overview of assay performance characteristics. Antivir. Ther. **5**:27–31.
32. **Salomon, H., A. Belmonte, K. Nguyen, Z. Gu, M. Gelfand, and M. A. Wainberg.** 1994. Comparison of cord blood and peripheral blood mononuclear cells as targets for viral isolation and drug sensitivity studies involving human immunodeficiency virus type 1. J. Clin. Microbiol. **32**:2000–2002.
33. **Sarmati, L., E. Nicastri, S. G. Parisi, G. d'Ettorre, G. Mancino, P. Narciso, V. Vullo, and M. Andreoni.** 2002. Discordance between genotypic and phenotypic drug resistance profiles in human immunodeficiency virus type 1 strains isolated from peripheral blood mononuclear cells. J. Clin. Microbiol. **40**:335–340.
34. **Shafer, R. W., M. J. Kozal, D. A. Katzenstein, W. H. Lipil, I. F. Johnstone, and T. C. Merigan.** 1993. Zidovudine susceptibility testing of human immunodeficiency virus type 1 (HIV) clinical isolates. J. Virol. Methods **41**:297–310.
35. **Shi, C., and J. W. Mellors.** 1997. A recombinant retroviral system for rapid in vivo analysis of human immunodeficiency virus type 1 susceptibility to reverse transcriptase inhibitors. Antimicrob. Agents Chemother. **41**:2781–2785.
36. **Soda, Y., N. Shimizu, A. Jinno, H. Y. Liu, K. Kanbe, T. Kitamura, and H. Hoshino.** 1999. Establishment of a new system for determination of coreceptor usages of HIV based on the human glioma NP-2 cell line. Biochem. Biophys. Res. Commun. **258**:313–321.
37. **Tamamura, H., Y. Xu, T. Hattori, X. Zhang, R. Arakaki, K. Kanbara, A. Omagari, A. Otaka, T. Ibuka, N. Yamamoto, H. Nakashima, and N. Fujii.** 1998. A low-molecular-weight inhibitor against the chemokine receptor CXCR4: a strong anti-HIV peptide T140. Biochem. Biophys. Res. Commun. **253**:877–882.

JOURNAL OF VIROLOGY, Jan. 2008, p. 764–774 Vol. 82, No. 2
0022-538X/08/$08.00+0 doi:10.1128/JVI.01534-07

Broad Antiretroviral Activity and Resistance Profile of the Novel Human Immunodeficiency Virus Integrase Inhibitor Elvitegravir (JTK-303/GS-9137)▽†

Kazuya Shimura,[1] Eiichi Kodama,[1]* Yasuko Sakagami,[1] Yuji Matsuzaki,[2] Wataru Watanabe,[2]‡ Kazunobu Yamataka,[2] Yasuo Watanabe,[2] Yoshitsugu Ohata,[2] Satoki Doi,[3] Motohide Sato,[2] Mitsuki Kano,[2] Satoru Ikeda,[2] and Masao Matsuoka[1]

Laboratory of Virus Immunology, Institute for Virus Research, Kyoto University, 53 Kawaramachi, Shogoin, Sakyo-ku, Kyoto 606-8507, Japan[1]; Japan Tobacco Inc., Central Pharmaceutical Research Institute, 1-1 Murasaki-cho, Takatsuki, Osaka 569-1125, Japan[2]; and Japan Tobacco Inc., Central Pharmaceutical Research Institute, Pharmaceutical Frontier Research Laboratories, 1-13-2 Fukuura, Kanazawa-Ku, Yokohama, Kanagawa 236-0004, Japan[3]

Received 13 July 2007/Accepted 22 October 2007

Integrase (IN), an essential enzyme of human immunodeficiency virus (HIV), is an attractive antiretroviral drug target. The antiviral activity and resistance profile in vitro of a novel IN inhibitor, elvitegravir (EVG) (also known as JTK-303/GS-9137), currently being developed for the treatment of HIV-1 infection are described. EVG blocked the integration of HIV-1 cDNA through the inhibition of DNA strand transfer. EVG inhibited the replication of HIV-1, including various subtypes and multiple-drug-resistant clinical isolates, and HIV-2 strains with a 50% effective concentration in the subnanomolar to nanomolar range. EVG-resistant variants were selected in two independent inductions, and a total of 8 amino acid substitutions in the catalytic core domain of IN were observed. Among the observed IN mutations, T66I and E92Q substitutions mainly contributed to EVG resistance. These two primary resistance mutations are located in the active site, and other secondary mutations identified are proximal to these primary mutations. The EVG-selected IN mutations, some of which represent novel IN inhibitor resistance mutations, conferred reduced susceptibility to other IN inhibitors, suggesting that a common mechanism is involved in resistance and potential cross-resistance. The replication capacity of EVG-resistant variants was significantly reduced relative to both wild-type virus and other IN inhibitor-resistant variants selected by L-870,810. EVG and L-870,810 both inhibited the replication of murine leukemia virus and simian immunodeficiency virus, suggesting that IN inhibitors bind to a conformationally conserved region of various retroviral IN enzymes and are an ideal drug for a range of retroviral infections.

Three unique and essential HIV enzymes, protease (PR), reverse transcriptase with RNase H (RT), and integrase (IN), appear to be ideal targets for the development of inhibitors of human immunodeficiency virus (HIV) replication. Anti-HIV drugs targeting PR (PR inhibitors [PIs]) and RT (nucleoside/nucleotide RT inhibitors [NRTIs] and nonnucleoside RT inhibitors [NNRTIs]) have been approved for use in the treatment of HIV infection. Combinations of these drugs used in highly active antiretroviral therapy can effectively suppress HIV replication in vivo to undetectable levels and have led to significant declines in HIV-associated mortality (28, 40). However, the emergence of drug-resistant HIV variants can attenuate the efficacy of antiretroviral treatment. Some primary infections also result from the transmission of HIV strains that possess drug-resistant genotypes and phenotypes (9). To suppress these drug-resistant variants, new anti-HIV drugs that block new targets are urgently needed.

IN, a 32-kDa protein resulting from the proteolytic cleavage of the *gag-pol* precursor, plays an essential role in the integration of proviral DNA into the host genome. As LaFemina et al. previously reported that there is no human homologue of HIV IN (31), it is an attractive target for the development of new antiretroviral therapeutic agents without adverse effects. IN consists of three domains: an N-terminal zinc finger domain and a C-terminal DNA-binding domain flank a central catalytic core domain (CCD) that plays a critical role in its enzymatic activity (13, 14). Following reverse transcription, IN exerts at least two functions: the cleavage of two conserved nucleotides from the 3′ ends of both strands of the viral cDNA (3′ processing) (1) and, subsequently, the ligation of the viral cDNA into the host genome (strand transfer) (14). Gap filling of the interfaces between the viral and host genomic DNA is then completed using the host DNA repair machinery via a mechanism that is not yet fully understood. The completion of integration results in a fully functional provirus, which can then be used to initiate viral DNA transcription.

Several compounds that inhibit IN activity have been described, including diketo acid (DKA) derivatives such as L-731,988 (24) and S-1360 (16), both of which have potent

* Corresponding author. Mailing address: Laboratory of Virus Immunology, Institute for Virus Research, Kyoto University, 53 Kawaramachi, Shogoin, Sakyo-ku, Kyoto 606-8507, Japan. Phone and fax: 81-75-751-3986. E-mail: ekodama@virus.kyoto-u.ac.jp.

† Supplemental material for this article may be found at http://jvi.asm.org/.

‡ Present address: Kyushu University of Health and Welfare, 1714-1 Yoshinomachi, Nobeoka, Miyazaki 882-8508, Japan.

▽ Published ahead of print on 31 October 2007.

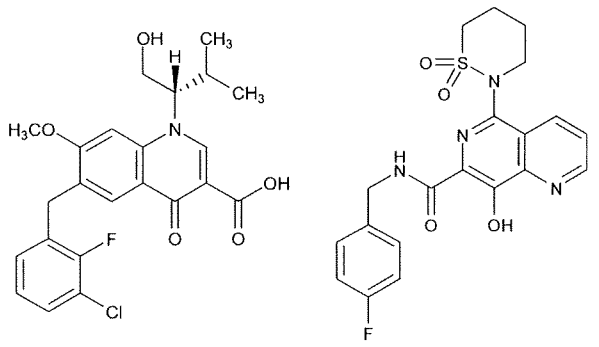

FIG. 1. Structure of EVG and L-870,810. A dihydroquinoline carboxylic acid derivative, EVG, and a naphthyridine carboxamide derivative, L-870,810 (a representative IN inhibitor), are shown.

antiviral activity. Crystal structure analysis has indicated that 1-(5-chloroindol-3-yl)-3-hydroxy-3-(2*H*-tetrazol-5-yl)-propenone, an S-1360 derivative, binds to the CCD, the putative active site of IN (19). In vitro resistance selection experiments with several IN inhibitors demonstrated that mutations in the CCD of IN play a significant role in the generation of IN inhibitor-resistant viral variants. In vitro selection of HIV-1 in the presence of the DKA IN inhibitors L-731,988 and S-1360 resulted in the emergence of viral variants carrying IN mutations associated with resistance. These mutations, including T66I, S153Y, and M154I, are located in close proximity to the catalytic triad residues (D64, D116, and E152) in the CCD of IN (16, 24). In contrast, L-870,810 (Fig. 1), which has previously demonstrated potent antiviral activity in HIV-1-infected patients in a monotherapy study (33), induced unique IN mutations, including V72I, F121Y, T125K, and V151I, when HIV was selected with the compound in vitro (23). These mutations are also located in the active site of IN, suggesting that a common mechanism may be involved in the acquisition of resistance to IN inhibitors.

Although no IN inhibitors are currently approved for clinical use (41), two IN inhibitors, elvitegravir (EVG) (formerly known as JTK-303/GS-9137, being codeveloped by Gilead Sciences and Japan Tobacco) (Fig. 1) (43, 56) and raltegravir (MK-0518, developed by Merck) (22), are currently being investigated in clinical studies of HIV-1-infected patients. In a phase II study, antiretroviral treatment-experienced patients using 125 mg EVG (boosted with ritonavir) along with an active optimized background regimen showed >2-$\log_{10}$ declines in their viral loads that were durable through week 24 (56).

Here, we describe the antiviral activity, mechanism of action, and resistance profile of EVG in vitro. EVG exerted potent anti-HIV activity against not only wild-type strains but also drug-resistant clinical isolates. Interestingly, EVG also showed antiviral activity against murine leukemia virus (MLV) and simian immunodeficiency virus (SIV). These results imply that IN inhibitors are ideal agents for the treatment of a range of retroviral infections. During the selection of EVG-resistant viral variants, novel IN mutations emerged. Combinations of these mutations conferred resistance to EVG and reduced susceptibility to other IN inhibitors, suggesting that there is a common mechanism underlying the resistance to IN inhibitors. One such mechanism may be conformational changes induced by multiple mutations located in the active site of IN.

MATERIALS AND METHODS

Antiviral agents. Zidovudine (AZT) and dextran sulfate (DS5000) (average molecular weight, 5,000) were purchased from Sigma (St. Louis, MO). Efavirenz (EFV) (NNRTI) and nelfinavir (NFV) (PI) were used for the control inhibitor. EVG (43), L-731,988 (42), L-870,810 (23), and S-1360 (16) were synthesized as described previously. The structures of EVG and L-870,810 are depicted in Fig. 1.

Cells and viruses. MT-2 and MT-4 cells were grown in RPMI 1640 medium. 293T cells were grown in Dulbecco's modified Eagle's medium. These media were supplemented with 10% fetal calf serum, 2 mM L-glutamine, 100 U/ml penicillin, and 50 μg/ml streptomycin. HeLa-CD4/CCR5-LTR/β-gal cells (5) were kindly provided by J. Overbaugh through the AIDS Research and Reference Reagent Program, Division of AIDS, National Institute of Allergy and Infectious Diseases (Bethesda, MD), and maintained in Dulbecco's modified Eagle's medium supplemented with 10% fetal calf serum, 200 μg/ml hygromycin B, 10 μg/ml puromycin, and 200 μg/ml geneticin. Peripheral blood mononuclear cells (PBMC) were obtained from healthy HIV-1-seronegative donors by centrifugation through Ficoll-Hypaque density gradients. PBMC were stimulated with 20 U/ml interleukin-2 (Shionogi, Osaka, Japan) and 0.5 μg/ml phytohemagglutinin (Sigma) for 3 days and then used for assays as described previously (30).

Three laboratory strains, HIV-1_{IIIB}, HIV-2_{EHO}, and HIV-2_{ROD}, were used in this study. Various subtypes of drug-naïve clinical isolates of HIV-1 (four isolates of subtype B and seven isolates of non-B subtypes) were employed. Four drug-resistant clinical isolates of HIV-1, including IVR401, IVR409, IVR411, and IVR415, were kindly provided by S. Oka (AIDS Clinical Center, International Medical Center of Japan, Tokyo, Japan).

Determination of HIV drug susceptibility. Inhibitory effects of compounds on HIV infection were determined using multinuclear activation of a galactosidase indicator (MAGI) assay, as previously described (37). Inhibitory effects on HIV-1 clinical isolates were measured by p24 production, and cytotoxicity was measured by using a 3-(4,5-dimethylthiazol-2-yl)-2,5-diphenyltetrazolium bromide (MTT) colorimetric assay, as described previously (30). Antiviral activities and cytotoxicities of inhibitors are presented as the concentrations that block viral replication by 50% (50% effective concentration [EC_{50}]) and that suppress the viability of target cells by 50%, respectively.

Quantification of HIV-1 DNA species. MT-2 cells (5×10^5 cells) were infected with HIV-1_{IIIB} at a multiplicity of infection (MOI) of 0.1 in the absence or presence of various inhibitors. Infected cells were washed after incubation for 2 h at 37°C. At 24 h postinfection, DNA was extracted using DNAzol reagent (Invitrogen, Carlsbad, CA).

Quantification of integrated HIV-1 DNA and the two-long-terminal-repeat (2-LTR) circle was performed by real-time quantitative PCR as described previously (4). To normalize DNA species among inhibitors, β-globin amplification was used as an internal control (51). Reactions were analyzed by using the ABI Prism 7500 sequence detector (PE Applied Biosystems, Foster City, CA), and results were then normalized and expressed as relative HIV-1 DNA species compared to a "no-inhibitor" control.

In vitro strand transfer assay. An oligonucleotide-based strand transfer assay was performed as previously described (8), with some modifications. Briefly, preprocessed oligonucleotide H-U5V1-2 (5′-ATGTGGAAAATCTCTAGCA-3′), derived from the U5 end of the HIV-1 LTR, was labeled at the 5′ end with [γ-^{32}P]ATP. Radiolabeled H-U5V1-2 was annealed to H-U5V2 (5′-ACTGCTA GAGATTTTCCACAT-3′) and then used for assays. Recombinant HIV-1 IN derived from HIV-1 NL4-3 (wild type) or EVG-selected mutants was prepared using an *Escherichia coli* expression system. The strand transfer assay was performed with 1 μM IN and 150 nM substrate DNA in 20 mM MOPS (morpholinepropanesulfonic acid) buffer with 30 mM $MgCl_2$ incubated in either the presence or absence of IN inhibitors at 37°C for 60 min. Reaction products were analyzed by electrophoresis on 25% polyacrylamide gels and quantified using a BAS-2500 imaging system (Fuji Photo Film, Tokyo, Japan). The concentration of IN inhibitor that inhibited the production of strand transfer products by 50% (50% inhibitory concentration [IC_{50}]) compared to the control was determined.

Selection of EVG-resistant HIV-1 variants in vitro. MT-2 cells (2×10^5 cells) were infected with HIV-1_{IIIB} and then cultured in the presence of 0.5 nM (see Fig. 3A) or 0.1 nM (see Fig. 3B) EVG. Cultures were incubated at 37°C until an

TABLE 1. Antiviral activities against laboratory HIV strains[a]

Strain	Mean EC_{50} (nM) ± SD		
	AZT	EVG	L-870,810
$HIV\text{-}1_{IIIB}$	7.1 ± 1.3	0.7 ± 0.3	6.3 ± 0.3
$HIV\text{-}2_{EHO}$	22 ± 9.1	2.8 ± 0.8	11 ± 1.9
$HIV\text{-}2_{ROD}$	19 ± 4.7	1.4 ± 0.7	8.6 ± 0.4

[a] Antiviral activity was determined using the MAGI assay. Data shown are means and standard deviations obtained from at least three independent experiments.

extensive cytopathic effect (CPE) was observed, and the culture supernatant was then harvested for further passage in fresh MT-2 cells. The concentration of EVG was increased when a significant CPE was observed. At the indicated passages (see Fig. 3A and B), proviral DNA was extracted from infected MT-2 cells and then subjected to PCR, followed by direct population-based sequencing. Susceptibility to EVG at the indicated passages was determined using the MAGI assay (see Fig. 3A) or p24 production (see Fig. 3B).

Recombinant HIV-1 clones. An HIV-1 infectious clone, pNL101 (38), kindly provided by K.-T. Jeang (NIH, Bethesda, MD), was used to generate recombinant HIV-1 clones. Wild-type HIV-1 ($HIV\text{-}1_{WT}$) was constructed by replacing the *pol* coding region (nucleotide positions 2006 of the ApaI site to 5122 of the NdeI site of pNL101) with HIV-1 strain BH10. The *pol* coding region contains a silent mutation at nucleotide 4232 (TTTAGA to TCTAGA) resulting in the generation of a unique XbaI site. Recombinant HIV-1 IN infectious clones were generated using a modified pNL101-based vector, $pNLRT_{WT}$. In brief, mutations were introduced into the XbaI-NdeI region (891 bp) of $pSLInt_{WT}$, which encodes nucleotides 4232 to 5122 of pNL101, using an oligonucleotide-based site-directed mutagenesis method (54). Next, the XbaI-NdeI fragments were inserted into pBNΔInt, which encodes nucleotides 5122 (NdeI) to 5785 (SalI) of pNL101. Finally, the XbaI-SalI region (1,554 bp) was inserted into pNL101. Each infectious clone was transfected into 293T cells. The following day, MT-2 cells were added, and the supernatants were harvested when an extensive CPE was observed.

Replication kinetics of resistant HIV-1 variants. MT-2 cells (10^5 cells) were infected with each virus preparation (500 MAGI units) for 4 h. The infected cells were then washed and cultured in the presence or absence of EVG. The culture supernatants were harvested on day 5 after infection, and p24 levels were quantified using a Retro-Tek HIV-1 p24 antigen enzyme-linked immunosorbent assay (ELISA) (ZeptoMetrix, Buffalo, NY).

Evaluation of antiretroviral activities of IN inhibitors. The MLV-based retroviral vector pRCV/LIG (15) and plasmid pcDNA-VSVG, encoding the vesicular stomatitis virus envelope glycoprotein (a generous gift from H. Miyoshi, RIKEN Bioresource Center, Tsukuba, Japan), were employed to generate viral particles. These plasmids were cotransfected into an MLV-derived Gag-Pol-expressing packaging cell line, GP293 (Clontech, Palo Alto, CA). After 48 h of transfection, culture supernatants were filtered through a 0.45-μm membrane and stored at −80°C until use.

An HIV-1-based luciferase expression vector, pBC-LIG; pCMVΔ8/9, encoding the HIV-1 viral proteins including IN; and pcDNA-VSVG were transfected into 293T cells to generate pseudotyped HIV-1. The viruses were used to infect 293T cells (10^5 cells per well in 12-well plates) at an MOI of 0.02 in the absence or presence of inhibitors. After 48 h of transduction, luciferase activity was determined using a luciferase assay system (Promega, Madison, WI) and an LB 9507 luminometer (Berthold, Bad Wildbad, Germany).

An SIV molecular clone, pMA239 (46), containing the full SIVmac239 genome, was a kind gift from E. Ido, Institute for Virus Research, Kyoto University. pMA239 was used to generate viral stocks as previously described (6). Antiviral activities of IN inhibitors against SIVmac239 were determined using the MAGI assay as described above.

Molecular modeling studies. A three-dimensional model of EVG in complex with HIV-1 IN CCD was prepared by PyMOL software, version 0.97, using previously reported data (44). Amino acid residues involved in resistance to EVG were displayed within this model.

RESULTS

Anti-HIV activities of IN inhibitors. The antiviral activity of EVG against $HIV\text{-}1_{IIIB}$, $HIV\text{-}2_{EHO}$, and $HIV\text{-}2_{ROD}$ was first evaluated by the MAGI assay. EVG showed potent antiviral activity against three laboratory strains of HIV, with EC_{50} values in the subnanomolar to nanomolar range (Table 1). Next, we evaluated the activity of EVG against wild-type clinical isolates representing various subtypes of HIV-1. EVG suppressed the replication of all HIV-1 subtypes tested, with an antiviral EC_{50} ranging from 0.10 to 1.26 nM (Table 2). Moreover, EVG suppressed the replication of HIV-1 clinical isolates carrying NRTI, NNRTI, and PI resistance-associated genotypes, as did a control IN inhibitor, the compound L-870,810 (see Table S1 in the supplemental material). The cytotoxicities of these inhibitors were also determined using an MTT colorimetric assay. Mean values for the concentration that suppresses the viability of target cells by 50% for EVG and L-870,810 in PBMC obtained from three independent donors were 4.6 ± 0.5 μM and 2.7 ± 0.6 μM, respectively. Thus, EVG can suppress various HIV strains, including diverse HIV-1 subtypes and clinical isolates carrying multiple mutations associated with resistance to currently approved antiretroviral drugs.

TABLE 2. Antiviral activities of EVG against various subtypes of HIV-1[a]

Subtype	Isolate	EC_{50} (nM)	
		AZT	EVG
A	RW/92/016	7.91	0.41
B	96USHIPS7	8.41	0.26
	BR/92/021	2.13	0.76
	BR/93/017	1.10	0.18
	BR/93/022	11.7	1.13
C	BR/92/025	2.84	0.10
D	UG/92/046	7.26	0.50
E	CMU02	9.07	1.26
F	BR/93/020	25.3	0.74
G	JV1083	11.1	0.35
O	BCF01	1.52	1.17

[a] Antiviral activity was determined using p24 ELISA.

Mechanism of anti-HIV activity of EVG. First, we performed a "time-of-addition" experiment as described previously (30), with some modifications. MT-4 cells were infected with $HIV\text{-}1_{IIIB}$ at an MOI of 0.5. One hour after infection, infected cells were extensively washed, and compounds were added, including an NNRTI (EFV at 100 nM), a PI (NFV at 500 nM), or EVG (100 nM). Amounts of p24 antigen were determined at 31 h postinfection. The antiviral activity of EFV gradually decreased from 6 h postinfection and disappeared at 12 h postinfection, whereas the antiviral activity of EVG decreased from 10 h postinfection and was no longer detected by 12 h postinfection. On the other hand, the PI NFV effectively blocked the infection up to 12 h postinfection and still exerted approximately 20% inhibitory activity up to 24 h postinfection. These results strongly suggest that EVG inhibits the HIV replication at a step that occurs after reverse transcription but before proteolytic cleavage, consistent with the integration step.

To elucidate the mode of action of EVG on HIV-1 replication, the levels of intracellular HIV-1 DNA species were determined using real-time quantitative PCR (Fig. 2A). MT-2 cells were infected with $HIV\text{-}1_{IIIB}$ in the presence or absence

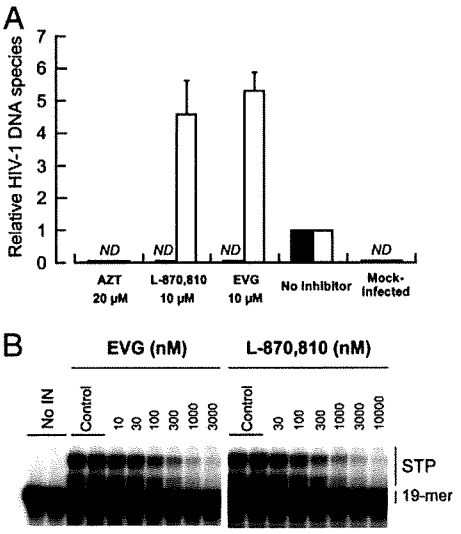

FIG. 2. Mechanism of action of EVG. (A) Quantification of HIV-1 DNA species. MT-2 cells were infected with HIV-1_{IIIB} in the presence or absence of AZT, L-870,810, and EVG. Unintegrated (2-LTR) (white bars) and integrated (black bars) forms of proviral DNA were quantified by real-time PCR and normalized to the β-globin gene after 24 h of infection. The data are represented as means and standard deviations of value relative to that of the no-inhibitor control from three independent experiments. ND means that the signals were not detected even after 40 cycles of amplification. (B) Inhibitory effect of IN inhibitors on strand transfer activity. Gel electrophoresis shows strand transfer products (STP) generated from preprocessed donor DNA substrate (19-mer) covalently bound to acceptor DNA.

of a CD4-gp120 binding inhibitor, DS5000; an NRTI, AZT; an IN inhibitor, L-870,810; and EVG. Unintegrated (2-LTR) and integrated forms of reverse-transcribed HIV-1 genomic DNA were quantified after 24 h of infection and then normalized with β-globin DNA. In the presence of 20 μM AZT, neither 2-LTR nor integrated forms were detected as expected. Similar results were also observed with 20 μM DS5000 (data not shown). In the presence of 10 μM L-870,810, integrated provirus was undetectable, while relative 2-LTR levels increased about 5-fold (4.6-fold ± 1.0-fold). Similar results were observed with 10 μM EVG (2-LTR) (5.3-fold ± 0.5-fold), indicating that EVG exerts anti-HIV activity by blocking the integration step.

To further characterize the mechanism by which EVG inhibits the integration step, the effect of EVG on strand transfer was assessed by characterizing its ability to inhibit the activity of recombinant wild-type HIV-1 IN enzyme in an oligonucleotide-based strand transfer assay (Fig. 2B). EVG and L-870,810 both inhibited the synthesis of strand transfer products with IC_{50} values of 54 nM and 118 nM, respectively. Taken together, these results indicate that like L-870,810, EVG blocks integration via the inhibition of IN-mediated strand transfer.

Selection of EVG-resistant HIV-1 variants in vitro. To determine the in vitro resistance profile of EVG, EVG-resistant viral variants were selected using a dose escalation method, and the susceptibilities of the resulting selected variants to EVG (EC_{50}) were determined. Selection of resistant HIV-1_{IIIB} was initiated with 0.5 nM EVG (Fig. 3A). At passage 12 (P-12), where the concentration of EVG was 4 nM, 2 amino acid substitutions, glutamine-to-proline at IN codon 146 (Q146P) and asparagine-to-aspartic acid at IN codon 232 (N232D), were observed (Fig. 3A). An N232D substitution was previously reported to be an IN polymorphism in HIV-1 (34). The EVG EC_{50} of a P-24 variant containing a Q146P- and N232D-substituted variant was 6.2 nM. At P-32 (32 nM EVG), a T66I IN substitution was newly observed, whereas the N232D substitution had reverted to the baseline sequence. The EVG EC_{50} against a P-36 variant was 64 nM. An S147G IN substitution was detected at P-48 (128 nM EVG), and the EVG EC_{50} further increased to 635 nM. In addition, a Q95Q/K IN substitution (mixture of Q and K) and an E138E/K IN substitution were newly identified at P-54 (256 nM EVG). These mixtures, Q95Q/K and E138E/K, fully emerged in the viral pools by P-64 and P-80, respectively. The EVG EC_{50} at P-68 (1,024 nM EVG) was greater than 1,000 nM.

An independent EVG selection experiment, again using HIV-1_{IIIB}, was performed but began at 0.1 nM EVG (Fig. 3B). An E92E/Q mixture in the IN coding region was first detected at P-30 (10 nM EVG) and was predominantly E92Q by P-38 (20 nM EVG). Additional IN substitutions, H51H/Y and S147S/G, emerged at P-60 (640 nM EVG), and an E157E/Q mixture emerged at P-70 (1,280 nM EVG); the viral pools at the terminal passage P-80 (1,280 nM EVG) had the IN sequence H51Y/E92Q/S147G/E157E/Q (Fig. 3B). The emergence of each of these mutations correlated with an increase in the EVG EC_{50} of the resulting viral pools (Fig. 3). Other than the N232D polymorphism, all of these mutations are located in the CCD of IN.

Phenotypic analysis of IN recombinant viruses. (i) EVG-selected mutations. To characterize which mutations are responsible for EVG resistance, infectious HIV-1 clones containing single IN substitutions (H51Y, T66I, E92Q, Q95K, E138K, Q146P, S147G, or E157Q) that were observed to emerge under selection with EVG were generated (Fig. 3 and Table 3). Mutations were classified into two groups based on the level of resistance: mutations that conferred more than 10-fold reduced susceptibility compared to the wild type were defined as primary mutations, and mutations conferring less than 10-fold reduced susceptibility were defined as secondary mutations. T66I and E92Q substitutions conferred significantly reduced susceptibility to EVG (37- and 36-fold reduced, respectively, relative to the wild type), whereas the Q146P and S147G substitutions conferred more moderate reductions in EVG susceptibility (11-fold reduced), indicating that these four IN mutations are primary mutations involved in resistance to EVG. In contrast, H51Y, Q95K, and E157Q substitutions all conferred smaller reductions in EVG susceptibility (each less than 6.3-fold reduced compared to the wild type), suggesting that these substitutions are secondary resistance mutations. Interestingly, the E138K mutation alone conferred no reduction in susceptibility to either EVG or L-870,810. Thus, several distinct mechanisms of resistance may be represented by these different IN mutations.

Multisubstituted clones observed during EVG selection experiments were also generated. HIV-$1_{T66I/Q146P}$ showed high-level resistance to EVG (119-fold reduced susceptibility) (Table 3). Combinations of S147G with T66I/Q146P or E92Q further enhanced resistance, 412- and 356-fold, respectively.

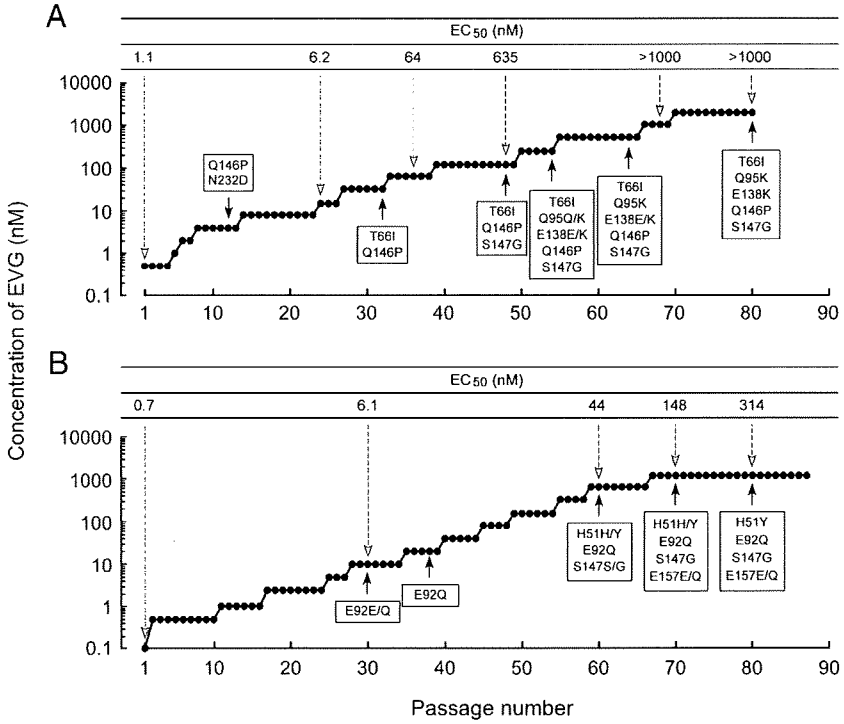

FIG. 3. Induction of EVG-resistant HIV-1. Data from MT-2 cells are shown. The initial concentrations of EVG were 0.5 nM (A) and 0.1 nM (B). Results are from two identical but independent experiments. At the indicated passage number (black arrowheads), proviral DNA extracted from infected MT-2 cells was sequenced. Amino acid substitutions are shown. The EC_{50} values of HIV-1 variants selected by EVG at the indicated passage number (white arrowheads) were determined using MAGI assay (A) or the production of p24 in MT-2 cells (B).

The triple mutant HIV-$1_{H51Y/E92Q/S147G}$ showed high-level resistance to EVG (700-fold reduced susceptibility). Interestingly, the addition of the secondary mutation H51Y, which on its own reduced EVG susceptibility only 3.6-fold, substantially enhanced resistance relative to that observed for the double mutant HIV-$1_{E92Q/S147G}$. HIV-$1_{T66I/Q95K/Q146P/S147G}$, HIV-$1_{T66I/Q95K/E138K/Q146P/S147G}$, and HIV-$1_{H51Y/E92Q/S147G/E157Q}$ mutants all showed high-level resistance to EVG, with EC_{50} values greater than 1,000 nM in all cases. These results indicate that the T66I and E92Q mutations provided the highest change (*n*-fold) in EVG susceptibility as individual resistance mutations and that the additional substitutions identified further enhance the level of resistance to EVG when combined with these primary mutations.

(ii) L-870,810-selected mutations. Infectious HIV-1 clones containing mutations (V72I, F121Y, T125K, and V151I) previously shown to be associated with resistance to L-870,810 (23) and two mutations, L74M and G163R, observed in our selection using L-870,810 (data not shown) were generated. Among these variants, HIV-1_{F121Y} and HIV-1_{V151I} demonstrated reduced susceptibility to both L-870,810 and EVG (Table 3). V151I has been observed in some HIV-1 clinical isolates and may be an IN polymorphism (34). Moreover, the effect of V151I on susceptibility to L-870,810 has been controversial (23, 29). This discrepancy might arise from the viral strain or plasmid backbone used, so further experiments to clarify the effect of V151I on IN inhibitor susceptibility are needed. HIV-$1_{F121Y/T125K}$ showed significant resistance to both L-870,810 and EVG (68-fold and 177-fold reduced susceptibility, respectively). HIV-$1_{V72I/F121Y/T125K/V151I}$ showed high-level resistance to both IN inhibitors (EC_{50} greater than 1,000 nM).

(iii) DKA IN inhibitor-selected mutations. Highlighting the potential for related mechanisms of IN inhibitor resistance and cross-resistance, the T66I mutation has also been observed to be selected by DKA IN inhibitors such as L-708,906 and S-1360. Additional mutations, L74M and S153Y, in combination with T66I were also observed to be selected by these DKA IN inhibitors (16, 17). L74M also emerged during L-870,810 selection in our studies (data not shown) but conferred no change in susceptibility to L-870,810 when present alone and only low-level resistance (3.0-fold) to EVG (Table 3). The combination of T66I and L74M conferred slightly higher resistance to EVG (45-fold) than did T66I alone but only moderate resistance to L-870,810 (7.1-fold). Another IN mutant, HIV-$1_{T66I/S153Y}$, observed in L-708,906 selection experiments (24) showed high-level resistance to EVG (260-fold) but low-level resistance to L-870,810 (5.0-fold). These results suggest that the mechanism of EVG resistance may have some similarities to that of DKA IN inhibitors.

Taken together, these results suggest that a variety of IN mutations may be selected by EVG and other IN inhibitors. Most of the IN inhibitor resistance mutations are observed to cluster in the CCD of IN. The resulting mutations and their combinations have the capacity to confer various levels of resistance and potential cross-resistance to EVG and other IN inhibitors. Given their location in the CCD, many of these mutations may act via a common mechanism. The observed development of IN inhibitor resistance mutations resembles

TABLE 3. Susceptibilities of HIV-1 IN recombinant molecular clones[a]

Molecular clone(s)	Mean EC_{50} (nM) ± SD (fold resistance compared to wild type)				
	AZT	EVG	L-870,810	S-1360	L-731,988
$HIV\text{-}1_{WT}$	32	1.1	5.8	1,239	736
EVG mutation (expt 1)[b]					
T66I[c]	43 ± 11 (1.3)	41 ± 14 (37)	4.7 ± 2.9 (0.8)	6,403 ± 2,349 (5.2)	7,234 ± 1,210 (9.8)
Q95K	34 ± 6 (1.1)	2.9 ± 0.4 (2.6)	18 ± 2 (3.1)	ND	ND
E138K	33 ± 8 (1.0)	1.1 ± 0.4 (1.0)	3.9 ± 0.4 (0.7)	ND	ND
Q146P	26 ± 2 (0.8)	12 ± 3 (11)	5.1 ± 0.4 (0.9)	ND	ND
S147G[d]	41 ± 5 (1.3)	12 ± 5 (11)	23 ± 6 (4.0)	ND	ND
T66I/Q146P	22 ± 2 (0.7)	131 ± 12 (119)	18 ± 5 (3.1)	ND	ND
T66I/Q146P/S147G	19 ± 5 (0.6)	453 ± 62 (412)	127 ± 37 (22)	ND	ND
T66I/Q95K/Q146P/S147G	31 ± 12 (1.0)	>1,000	303 ± 76 (52)	ND	ND
T66I/Q95K/E138K/Q146P/S147G	41 ± 7 (1.3)	>1,000	306 ± 76 (53)	>10,000	>50,000
EVG mutation (expt 2)[b]					
H51Y	34 ± 8 (1.1)	4.0 ± 0.6 (3.6)	3.3 ± 0.7 (0.6)	ND	ND
E92Q	32 ± 4 (1.0)	40 ± 12 (36)	63 ± 39 (11)	ND	ND
E157Q	34 ± 8 (1.1)	6.9 ± 1.4 (6.3)	52 ± 20 (9.0)	ND	ND
E92Q/S147G	39 ± 9 (1.2)	392 ± 133 (356)	587 ± 64 (101)	ND	ND
H51Y/E92Q/S147G	54 ± 6 (1.7)	769 ± 88 (699)	374 ± 100 (64)	>10,000	22,175 ± 1,299 (30)
H51Y/E92Q/S147G/E157Q	21 ± 2 (0.7)	>1,000	340 ± 26 (59)	>10,000	18,652 ± 4,575 (25)
L-870,810 mutation					
V72I	17 ± 1 (0.5)	4.3 ± 1.1 (3.9)	9.1 ± 2.5 (1.6)	ND	ND
L74M[c]	20 ± 3 (0.6)	3.3 ± 1.1 (3.0)	4.4 ± 1.7 (0.8)	1,500 ± 302 (1.2)	4,471 ± 942 (6.1)
F121Y	15 ± 1 (0.5)	28 ± 11 (25)	51 ± 23 (8.8)	ND	ND
T125K	17 ± 3 (0.5)	2.3 ± 1.1 (2.1)	9.9 ± 3.7 (1.7)	ND	ND
V151I	21 ± 4 (0.7)	11 ± 3 (10)	104 ± 29 (18)	ND	ND
G163R	22 ± 7 (0.7)	0.8 ± 0.2 (0.7)	6.5 ± 2.6 (1.1)	ND	ND
F121Y/G163R	36 ± 5 (1.1)	60 ± 20 (55)	219 ± 20 (38)	ND	ND
F121Y/T125K	38 ± 12 (1.2)	195 ± 73 (177)	393 ± 82 (68)	ND	ND
V72I/F121Y/T125K	33 ± 7 (1.0)	143 ± 25 (130)	886 ± 79 (153)	ND	ND
V72I/F121Y/T125K/V151I	64 ± 9 (2.0)	>1,000	>1,000	>10,000	>50,000
DKA mutation					
T66I/L74M	46 ± 11 (1.4)	49 ± 5 (45)	41 ± 10 (7.1)	>10,000	23,043 ± 4,886 (31)
T66I/S153Y	26 ± 8 (0.8)	285 ± 63 (259)	29 ± 9 (5.0)	>10,000	8,478 ± 1,267 (12)

[a] Antiviral activity was determined using the MAGI assay. Data shown are means and standard deviations obtained from at least three independent experiments, and resistance (*n*-fold) of the EC_{50} of the IN recombinant molecular clone compared to that of parental $HIV\text{-}1_{WT}$ is shown in parentheses. ND, not determined.
[b] EVG selection was performed in two independent experiments, and observed mutations are separately represented.
[c] Also observed in the DKA selected mutation.
[d] Observed in two independent EVG-selected experiments.

that seen for other antiretroviral drugs such as PIs; i.e., multiple mutations are introduced in a stepwise fashion and are required for high-level resistance to the selecting inhibitors (10, 50).

Strand transfer assay. To further characterize the effect of EVG-selected resistance mutations on IN function, the effect of mutations on the enzymatic activity of recombinant IN was evaluated in an in vitro strand transfer assay (Fig. 4). IN enzymes carrying the individual mutations H51Y, S147G, and E157Q had reduced strand transfer activity relative to that of the wild type (57%, 36%, and 79% of wild-type levels, respectively). Strand transfer activities of E92Q, E92Q/S147G, and H51Y/E92Q/S147G IN enzymes decreased with the accumulation of mutations from 57% to 29 and 22% of the wild type, respectively. However, the introduction of E157Q to H51Y/E92Q/S147Q partially restored strand transfer activity to 46% of wild-type activity, suggesting that E157Q may play a role in compensating for the loss of strand transfer activity resulting from the emergence of EVG resistance mutations.

The effect of EVG-selected mutations on the inhibition of strand transfer by EVG and L-870,810 was also determined (Fig. 4). Recombinant IN enzymes carrying the individual H51Y, S147G, and E157Q substitutions remained susceptible to both EVG and L-870,810 (0.7- to 2.1-fold reduced susceptibility). E92Q IN demonstrated only moderate resistance to both IN inhibitors in the strand transfer assay (4.3-fold reduced for both inhibitors). The combination of E92Q and S147G enhanced resistance to both EVG and L-870,810 (7.6- and 8.5-fold reduced susceptibility, respectively). However, unlike the IN recombinant viruses in the antiviral assay, neither the H51Y/E92Q/S147G nor the H51Y/E92Q/S147G/E157Q IN enzymes showed further enhancement of resistance in the strand transfer assay. This difference in results from the strand transfer assay versus those from the antiviral assay may reflect differences in the recombinant IN enzyme versus the viral IN enzyme in situ. Indeed, structure-activity relationship experiments described in a previous report (43) revealed that antiviral activity and in vitro enzyme inhibition were well correlated. Nevertheless, this biochemical analysis confirmed that the E92Q IN mutation confers significantly reduced suscepti-